WSRC-STI-2006-00221
Revision 1

Key Words:
Electrolysis (HTE)
High Average Power Laser (HAPL)
High Temperature
Hybrid Sulfur (HyS)
Hydrogen
Laser Inertial Fusion Energy (IFE)
Sulfur-Iodine (SI)
Thermochemical
Water-splitting

Retention: Permanent

FEASIBILITY OF HYDROGEN PRODUCTION USING LASER INERTIAL FUSION AS THE PRIMARY ENERGY SOURCE (U)

Maximilian B. Gorensek

NOVEMBER 3, 2006

Washington Savannah River Company
Savannah River Site
Aiken, SC 29808

Prepared for the U.S. Department of Energy
Under Contract Number DEAC09-96-SR18500

SRNL
SAVANNAH RIVER NATIONAL LABORATORY

DISCLAIMER

Printed in the United States of America

Prepared For
U.S. Department of Energy

REVIEWS AND APPROVALS

Maximilian B. Gorensek, Author, Computational and Statistical Science	Date
Melvin R. Buckner, Technical Reviewer, Energy Security	Date
Steven J. Hensel, Manager, Computational and Statistical Science	Date
William A. Summers, Hydrogen Program Manager, Energy Security	Date
Benjamin J. Cross, Nuclear Energy Program Manager, Energy Security	Date
Paul F. Cloessner, Manager, Homeland and National Security	Date

TABLE OF CONTENTS

LIST OF TABLES v

LIST OF FIGURES v

LIST OF ACRONYMS vi

EXECUTIVE SUMMARY 1

1.0 INTRODUCTION 2
1.1 The HAPL Program 2
1.2 Hydrogen Production from Fusion Energy 4

2.0 PURPOSE 6

3.0 LASER IFE HEAT TRANSFER CONSIDERATIONS 7
3.1 Helium-cooled Vs. Self-cooled Blankets 7
3.2 Factors Affecting Temperature Ranges of Blanket Materials 7
3.3 HAPL Self-cooled Blanket Conceptual Designs 9
3.4 Helium-cooled Blanket Concepts 15
3.5 Dual-cooled Blanket Concepts 16
3.6 Advanced Blanket Concepts 18
3.7 Blanket Concepts Evaluated 19

4.0 THEORETICAL EFFICIENCY LIMITS 20
4.1 Ideal Net Thermal Efficiency for a Water-splitting Process 20
4.2 Net Thermal Efficiency Estimates for HAPL 22

5.0 WATER-SPLITTING OPTIONS FOR HAPL 25
5.1 Thermochemical Cycles 26
5.1.1 Sulfur-Iodine Cycle 27
5.1.2 Hybrid Sulfur Cycle 31
5.1.3 Other Cycles 34
5.2 High Temperature Electrolysis 35
5.3 Proposed Water-splitting Options for HAPL 38

6.0 THE CASE FOR LASER IFE HYDROGEN PRODUCTION 39
6.1 Temperature Considerations 39
6.2 Heat Transfer Considerations 41
6.3 Materials Considerations 42

7.0 SUITABILITY OF FTF FOR HYDROGEN PRODUCTION DEMONSTRATION 44

8.0 CONCLUSIONS AND RECOMMENDATIONS 45

9.0 REFERENCES 46

LIST OF TABLES

Table 3-1 Selected Parameters for FS HAPL Chamber with Self-cooled Li Blanket [Sviatoslavsky et al. (2005)] 10
Table 3-2 Key design parameters of eight advanced FW/blanket designs [Wong et al. (2002)] 18
Table 4-1 Net Thermal Efficiency Estimates for HAPL Blanket Concepts 22
Table 4-2 Comparison between Net Thermal Efficiencies for High Temperature Water-splitting Versus Electrolysis 24
Table 5-1 Thermodynamics of the Water-splitting Reaction 25

LIST OF FIGURES

Figure 1-1 HAPL Laser Fusion Energy Power Plant Schematic [UCSD (2006)] 3
Figure 3-1 Impact of Fusion Reaction on Reaction Chamber Wall [Obenschain (2006)] 8
Figure 3-2 Cross-section of FS HAPL Chamber with Self-cooled Li Blanket [Sviatoslavsky et al. (2005)] 10
Figure 3-3 Side Blanket Module [Sviatoslavsky et al. (2005)] 11
Figure 3-4 Cross-sections of a Side Blanket Sub-module [Sviatoslavsky et al. (2005)] 11
Figure 3-5 Cross-section of SiC_f/SiC HAPL Chamber with Magnetic Diversion and Self-cooled Pb-17Li Blanket [Raffray (2006)] 13
Figure 3-6 Chamber Cross-section with Magnetic Diversion [Sviatoslavsky (2006)] 13
Figure 3-7 Mid Blanket Module [Sviatoslavsky (2006)] 14
Figure 3-8 Mid Blanket Sub-module [Sviatoslavsky (2006)] 14
Figure 3-9 Helium-cooled Ceramic Breeder Concept (HCPB) [Diegele (2002)] 16
Figure 3-10 ARIES Dual-cooled Lead-lithium Blanket Concept [Tillack et al. (2003)] 17
Figure 3-11 Typical Dual-cooled Lead-lithium Flow Cell [Morley et al. (2005)] 17
Figure 4-1 Simplified Water-splitting Hydrogen Production Process 21
Figure 5-1 Sulfur-Iodine Cycle Schematic Diagram 27
Figure 5-2 Simplified Flowsheet of Laser IFE-driven SI Cycle Process [adapted from Summers (2006)] 28
Figure 5-3 Hybrid Sulfur Cycle Schematic Diagram 32
Figure 5-4 Simplified Block Flowsheet of Laser IFE-driven HyS Cycle Process 33
Figure 5-5 High Temperature Steam Electrolysis Cell Schematic [DOE (2004)] 36
Figure 5-6 Simplified Flowsheet of Laser IFE-driven High Temperature Electrolysis Process [adapted from DOE (2004)] 37
Figure 6-1 SNL SiC H_2SO_4 Decomposition Reactor Concept [Evans (2006)] 42

LIST OF ACRONYMS

Ca-Br	Calcium-Bromine (cycle)
DEMO	ITER experiemnt Demonstration Reactor
DT	Deuterium-Tritium
DOE	United States Department of Energy
DOE-NE	United States Department of Energy, Office of Nuclear Energy, Science & Technology
Flibe	34% BeF_2, 66% LiF salt mixture
FLiNaK	46.5% LiF, 11.5% NaF, 42% KF salt mixture
FS	Ferritic Steel
FTF	Fusion Test Facility
FW	First Wall
GA	General Atomics Corporation
H_2	Hydrogen
H2-MHR	Hydrogen Modular Helium Reactor
H_2O	Water
HAPL	High Average Power Laser
HCPB	Helium-Cooled Pebble Bed
HI	Hydrogen Iodide
HHV	Higher Heating Value
HTE	High Temperature Electrolysis
HyS	Hybrid Sulfur (cycle)
IFE	Inertial Fusion Energy
IHX	Intermediate Heat Exchanger
I-NERI	International Nuclear Energy Research Initiative
I_2	Iodine
ITER	International Thermonuclear Experimental Reactor
JAEA	Japanese Atomic Energy Agency
Li	Lithium
LLNL	Lawrence Livermore National Laboratory
NHI	Nuclear Hydrogen Initiative
NRC	National Research Council
NRL	Naval Research Laboratory
$O^=$	Oxide anion
O_2	Oxygen
ODS	Oxide Dispersion-Stabilized
Pb-17Li	83% lead, 17% lithium eutectic alloy
PEM	Proton Exchange Membrane
PPPL	Princeton Plasma Physics Laboratory
R&D	Research and Development
RWTH	Rheinisch-Westfälische Technische Hochschule (Rhine-Westphalian University of Technology)
SDE	SO_2-Depolarized Electrolysis
SI	Sulfur-Iodine (cycle)

SiC	Silicon Carbide
SiC_f/SiC	Silicon-Carbide-fiber-reinforced Silicon-Carbide-matrix composite
SNL	Sandia National Laboratories
SO_2	Sulfur Dioxide
SRNL	Savannah River National Laboratory
UCSD	University of California, San Diego
UT-3	University of Tokyo – 3
WNA	World Nuclear Association

EXECUTIVE SUMMARY

The High Average Power Laser (HAPL) program is developing technology for Laser IFE with the goal of producing electricity from the heat generated by the implosion of deuterium-tritium (DT) targets. Alternatively, the Laser IFE device could be coupled to a hydrogen generation system where the heat would be used as input to a water-splitting process to produce hydrogen and oxygen. The production of hydrogen in addition to electricity would allow fusion energy plants to address a much wider segment of energy needs, including transportation.

Water-splitting processes involving direct and hybrid thermochemical cycles and high temperature electrolysis are currently being developed as means to produce hydrogen from high temperature nuclear fission reactors and solar central receivers. This paper explores the feasibility of this concept for integration with a Laser IFE plant, and it looks at potential modifications to make this approach more attractive. Of particular interest are: 1) the determination of the advantages of Laser IFE hydrogen production compared to other hydrogen production concepts, and 2) whether a facility of the size of FTF would be suitable for hydrogen production.

1.0 INTRODUCTION

About three-fifths of the total energy usage in the United States of America occurs in the transportation and industrial sectors [DOE (2006)]. Most of this consumption is in the form of hydrocarbon fuels derived from petroleum and natural gas, of which an ever-increasing fraction is imported. Combustion of these fuels releases huge quantities of carbon dioxide, a greenhouse gas that is suspected of causing global warming. Hydrogen is being promoted as an alternative fuel because it can be made from water, which is ubiquitous, and because it can be used in fuel cells to make electric power efficiently while releasing only water vapor to the atmosphere. The widespread use of hydrogen as a fuel instead of hydrocarbons has the potential to reduce carbon dioxide emissions from both transportation and industrial applications and to reduce our national dependence on imported fuels [NRC (2004)]. However, in order to achieve these attributes, the hydrogen will need to be produced from domestic resources in processes that do not release greenhouse gases. This white paper addresses the feasibility of using Laser IFE to split water and produce hydrogen on a massive scale. In particular, it evaluates the potential of the conceptual designs that have been developed for the HAPL program for efficient, practical hydrogen production.

1.1 The HAPL Program

The HAPL program is a multi-institutional effort to develop a viable fusion energy source based on Laser IFE technology that is funded by the United States Department of Energy (DOE) and administered through the Naval Research Laboratory (NRL) in collaboration with the Lawrence Livermore National Laboratory (LLNL) [Sethian et al. (2003)]. A schematic of the HAPL conceptual design is illustrated in Figure 1-1 below.

In the HAPL concept, a spherical cryogenic target containing a DT mixture is periodically (5 Hz) injected into the center of a reaction chamber where it is symmetrically illuminated by an array of intense lasers. This causes the target to implode and heat up so rapidly and intensely that it undergoes thermonuclear burn. The deuterium and tritium nuclei fuse to produce helium and energetic neutrons:

$$^2H + ^3H \rightarrow ^4He(3.5MeV) + n(14.1MeV)\,.$$

All of the energy released by the fusion reaction is recovered by the chamber wall and the breeder blanket surrounding it. Most of it is carried by the neutrons, which heat the blanket through collisions with the constituent atoms. The neutrons ultimately react with the nuclei of lithium atoms in the blanket to make (or "breed") more tritium, which does not occur naturally and is needed to fuel the fusion reaction:

$$n + ^6Li \rightarrow ^3H + ^4He\,,$$
$$n + ^7Li \rightarrow ^3H + ^4He + n\,.$$

The tritium and helium products are removed from the blanket and the recovered heat is used to drive an electric power plant.

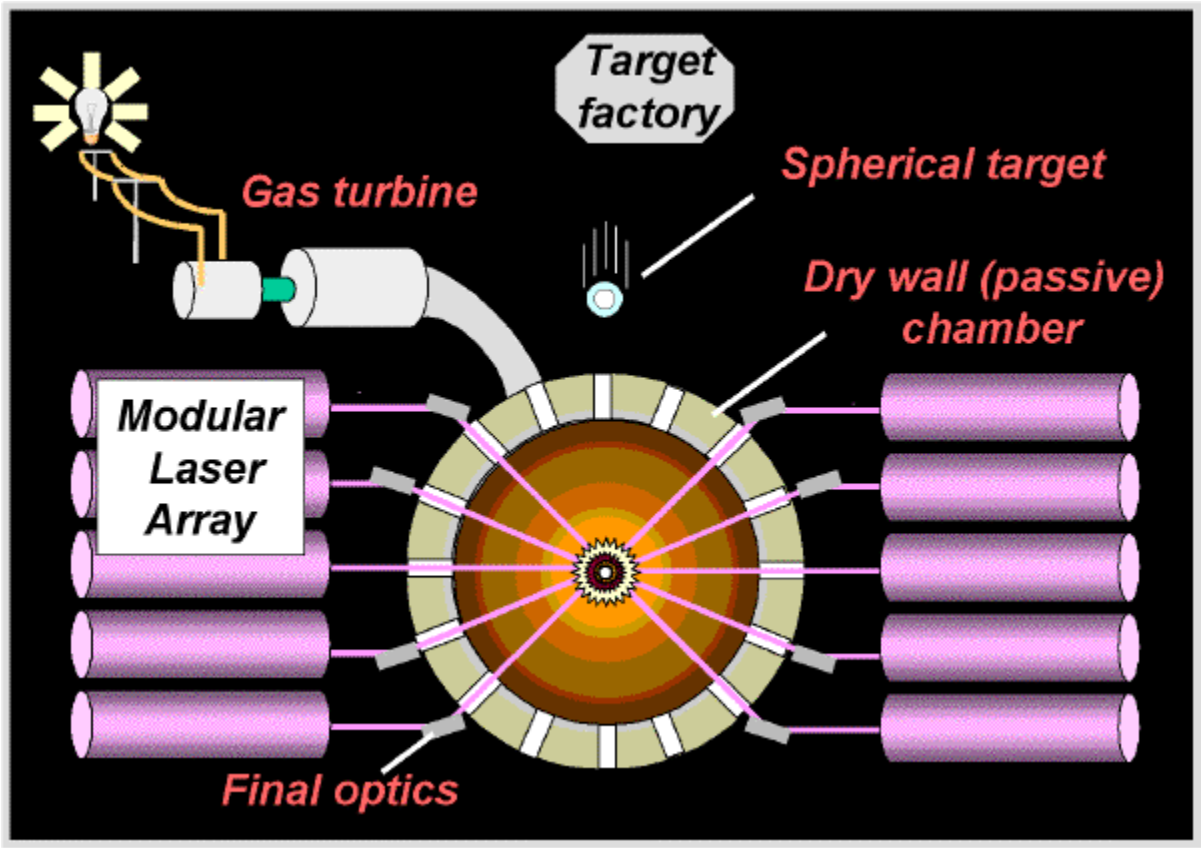

Figure 1-1 HAPL Laser Fusion Energy Power Plant Schematic [UCSD (2006)]

What makes HAPL attractive is its relative simplicity and its separable and modular architecture [UCSD (2006)]. The DT targets can be made in a single droplet generator using an automated, low-cost, process. Since the first wall (FW) is passive and does not have to hold a vacuum, it can be made in individual sections that can be replaced as needed. A wider range of material choices for the FW, including advanced composites and two-component structures, is also made possible by eliminating the vacuum integrity requirement. The power plant can be developed and tested separately from the fusion process, lowering development costs. Finally, the modular laser would consist of twenty-to-forty identical parallel beam lines, making it possible to develop the entire system by developing only one of these lines. This also reduces development costs significantly.

The HAPL program has been divided into three distinct phases with increasing confidence, decreasing technical risk, and increasing cost at each step. The first phase, expected to be complete by 2008, is development of the critical technologies needed for Laser IFE. Full-size components will be developed, tested, and integrated during the second phase, which is expected to last until 2013-14. The third phase will see the construction, operation, and testing of a demonstration fusion energy plant, originally conceived as a 300-to-700-MW_e net Experimental Test Facility (ETF) operating by 2020 [Sethian and Obenschain (2003)]. This has recently been scaled back to a 150-MW_{th} Fusion Test Facility (FTF) that could be running by 2018 [Sethian and Obenschain (2005)]. HAPL is ultimately directed toward the

design, construction, and operation of a full-scale Laser IFE power plant in the mid-to-late 2020s. The FTF will be used to evaluate and resolve the technologies that will be used in this Laser IFE system [Sethian (2006)].

1.2 Hydrogen Production from Fusion Energy

Hydrogen is analogous to electricity in that it is not an energy source, since neither occurs naturally in usable form. Both require a primary energy source and a conversion process that can transform that energy into either electric current or hydrogen fuel. In that sense, both hydrogen and electricity can be regarded as energy currencies [Scott (1994)]. Hydrogen has the advantage over electricity in that it can be used as fuel for either internal combustion engines or fuel cells to directly replace petroleum use in the transportation sector. Battery-powered electric vehicles have been shown to have limited capability to impact transportation energy use, although plug-in hybrid vehicles have been proposed as a future technology that may be more successful. However, hydrogen fuel cell vehicles are the primary focus of the DOE Energy Efficiency Office for development of future transportation technology. President Bush announced a Presidential Hydrogen Fuel Initiative in his 2003 State of the Union speech that established this as a national goal.

Fusion energy is being developed for the most part as a sustainable primary source to generate electricity. For example, the focus of the ITER international fusion experiment is on developing technology that can take today's plasma physics experiments and build them up to a demonstration power plant producing 1,000 MW of electricity by 2035 [PPPL (2006)]. As stated on the ITER web site home page, "fusion research is aimed at demonstrating that this energy source can be used to produce electricity in a safe and environmentally benign way..." [ITER (2006)]. Similarly, the HAPL program has as its objective "to develop the science and technology for … Laser IFE … (such that the) energy released is recovered … and converted into electricity" [UCSD (2006)]. A key step in the HAPL development path will be the FTF, which could be considered comparable to the small fission reactors that were built and tested before the first fission power plants were commercialized. The intent of the FTF is to serve as a test bed for fusion power plant materials and components [Obenschain et al. (2006)].

If fusion energy can be converted into electric energy currency, then it would be logical to consider the alternative possibility of converting it into hydrogen energy currency as well. Such is the case with DOE's Generation IV fission reactor development program, which includes not only the development of advanced power conversion technologies that can be coupled with fourth-generation fission reactors, but also allows for the development of hydrogen production technologies [DOE (2002)]. Indeed, the Nuclear Hydrogen Initiative (NHI) was created by the DOE with the intent of supporting the President's Hydrogen Fuel Initiative by developing hydrogen production technology that could be deployed with Generation IV fission reactors [DOE (2004)].

The temperature ranges over which heat transfer from the fusion reactor to the power conversion unit is being proposed in the HAPL program are comparable to the primary and secondary coolant temperature ranges that have been established for Generation IV fission reactors (850-1000°C). This suggests that a fusion-powered hydrogen fuel plant should be

considered as a viable alternative to a fission-powered hydrogen fuel plant or a fusion-powered electric generating plant.

2.0 PURPOSE

The HAPL program is developing technology for Laser IFE with the goal of producing electricity from the heat generated by the implosion of DT targets. The heat created by the Laser IFE device could also be used for thermochemical splitting or high-temperature electrolysis of water in a hydrogen production process. The Naval Research Laboratory (NRL) has tasked the Savannah River National Laboratory (SRNL) with preparing a white paper that explores the feasibility of using Laser IFE to produce hydrogen by means of water-splitting. Besides assessing the practicality of fusion-powered hydrogen production, this document considers and evaluates potential modifications to make this approach more attractive. Two particular questions that the white paper addresses are:

1. Does Laser IFE afford any advantages over other potential hydrogen production concepts, particularly those using nuclear fission as the primary energy source?

2. Is the proposed size of the FTF suitable for a hydrogen production demonstration?

3.0 LASER IFE HEAT TRANSFER CONSIDERATIONS

As noted in the description of the HAPL concept in the introduction, the energy of the fusion reaction will ultimately be collected by the breeder blanket in the form of heat. The ways in which this heat can be removed from the blanket and transferred to the water-splitting process will determine whether hydrogen production is feasible. The single most important variable is the temperature at which this heat can be transferred. A variety of blanket materials and cooling configurations has been proposed. These can be subdivided into solid, helium-cooled and fluid, self-cooled, as well as dual-cooled (both helium- and self-cooled) categories.

3.1 Helium-cooled Vs. Self-cooled Blankets

A solid, fixed blanket would obviously be constrained to remain in the chamber wall. For example, the blanket could be made out of a ceramic material containing some quantity of lithium for tritium breeding purposes. The heat recovered from the fusion process would then have to be transferred to the power- or hydrogen production-plant by means of a recirculating coolant loop containing helium gas under high pressure. This helium could be used directly in the hydrogen production plant, or its energy could be transferred to a secondary coolant loop though an intermediate heat exchanger. The necessity of using a secondary coolant needs to be evaluated based on regulatory, technical, economic and safety considerations.

A self-cooled blanket, on the other hand, would not remain in the chamber wall, but would circulate between the reaction chamber and the power plant. This category is obviously limited to fluid materials. Molten lithium salts or liquid lithium metal would be good examples. The heat produced by the fusion process would be removed by heat transfer from the primary coolant to a secondary coolant through the use of an intermediate heat exchanger. Heat from the secondary coolant would then by used to power a hydrogen production plant. Direct use of the primary coolant to power the hydrogen plant could also be studied, but this is considered an undesirable approach for most self-cooled blanket materials of interest due to safety and technical considerations, such as the high reactivity of lithium metal with aqueous streams.

While blanket materials from both categories (and even some dual-cooled options) are being considered for use in the HAPL program, only self-cooled blankets have been evaluated in conceptual designs so far. However, helium- and dual-cooled breeder blanket conceptual designs have been prepared for other fusion power sources. This exercise will consider all possible HAPL blanket and cooling options and their effect on hydrogen production.

3.2 Factors Affecting Temperature Ranges of Blanket Materials

A simple schematic of the impact of the fusion reaction on the reaction chamber wall is depicted in Figure 3-1 [Obenschain (2006)]. Each target fusion reaction releases an intense burst of energy. Nearly 30% of this energy strikes the wall in the form of ions, with another 1% arriving as x-ray photons. The balance, about 70%, hits the wall as energetic neutrons.

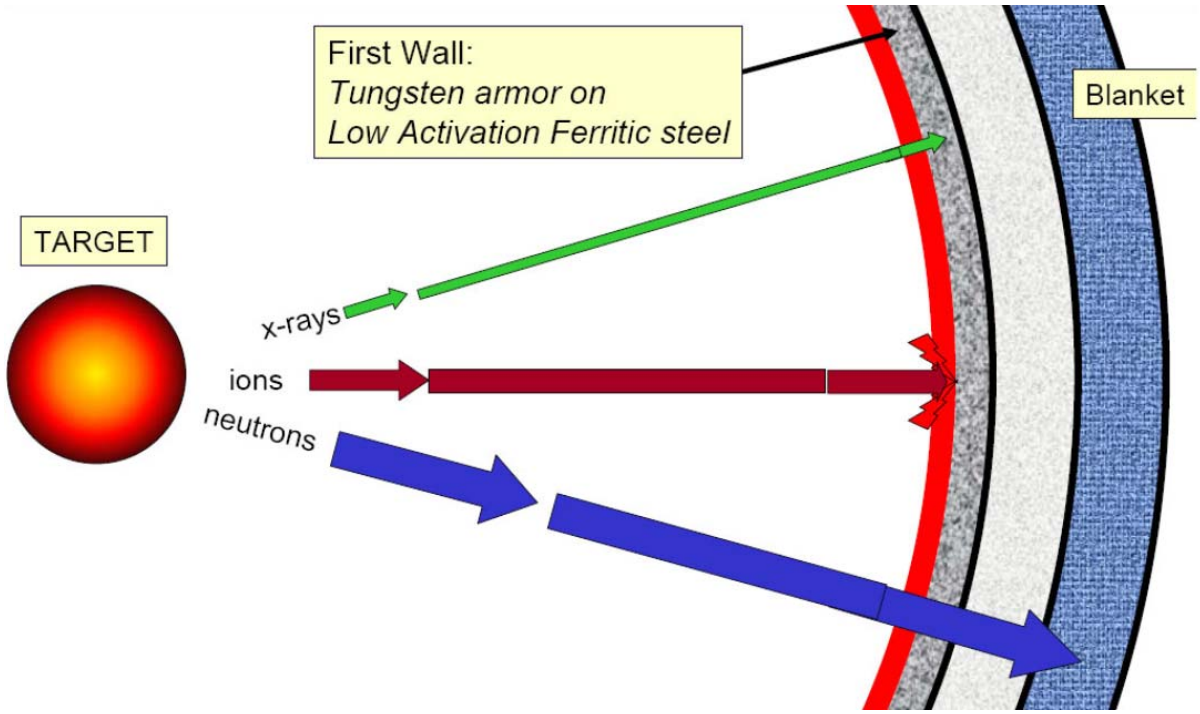

Figure 3-1 Impact of Fusion Reaction on Reaction Chamber Wall [Obenschain (2006)]

The ions represent a major threat to the integrity of the wall. Together with the x-ray photons, they penetrate no deeper than 10-100 μm and release their energy throughout this shallow depth. The result is intense heating very close to the surface. (The neutrons penetrate all the way through to the blanket, so they do not pose a threat to the FW.) Due to the periodic nature of the Laser IFE process (5-Hz target fusion frequency), the temperature near the surface of the FW is cyclic. In order to use a ferritic steel (FS) as the structural material for the FW, it would need to be covered with a protective coating that could withstand these surface temperature excursions. Furthermore, the diameter of the reaction chamber would have to be large enough to keep the peak surface temperature below the useful life-limiting temperature of the protective coating. Finally, FS can be severely corroded by molten metals and salts above certain temperatures. Consequently, the interface between the self-cooled blanket and the FS FW structure would have to be kept at a temperature below the corrosion limit.

The operating temperature range of a self-cooled blanket will be determined by the blanket-FW interface temperature limit and by the neutronics and thermal hydraulics of the blanket itself. Since the blanket will be heated primarily by neutron absorption, its internal temperature could actually be significantly hotter than the temperature of its interface with the FW. Using a ceramic material like silicon carbide (SiC) in place of FS would raise the blanket-FW interface temperature limit and allow the self-cooled blanket to operate over a higher temperature range.

Ionic bombardment of the FW could be mitigated through the use of magnetic diversion. This would involve the application of a magnetic field to the reaction chamber in a cusp configuration, diverting the energetic ion flux to ion collectors or dumps. As the ions would

expand they would perform work on the field, converting kinetic to electromagnetic energy. The FW could no longer be metallic because a conductive wall would return the energy back to the ions without dissipation. An insulating FW with a resistive blanket would be ideal, because most of the ions' energy would then be dissipated resistively in the blanket. If a resistive material like SiC were to be used for the FW instead, the dissipation would occur in the FW. In either case, by the time the ions would reach the dump, they would have exhausted much of their potential for damage. Although this would introduce an extra degree of complexity to Laser IFE, it also offers the promise of smaller reaction chambers.

3.3 HAPL Self-cooled Blanket Conceptual Designs

Two conceptual designs for self-cooled blankets have been prepared for the HAPL program to date. One uses a liquid lithium blanket in conjunction with a tungsten-armored FS FW [Sviatoslavsky et al. (2005)]. The other involves magnetic diversion, using liquid 83% lead-17% lithium eutectic alloy (Pb-17Li) for the blanket and SiC-fiber-reinforced SiC-matrix (SiC_f/SiC) composite for the FW [Sviatoslavsky (2006), Raffray (2006)].

The first design is illustrated in Figure 3-2 below. The FW and side blanket are barrel-shaped with a maximum radius of 6.5 m, tapering to 2.5 m at the extremities. Twelve modules extending the height of the chamber comprise the side blanket, each subtending 30° of circumference. (See Figure 3-3.) Separate blankets cover the upper and lower extremities. Coolant connections to the blanket are made at the bottom of the chamber. Cradles attached to the vacuum vessel support the side modules. The vacuum vessel also supports the upper and lower blankets sections. Beam tubes for sixty lasers terminate at the vacuum vessel wall, from where individual laser beams pass through ports in the blanket to converge in the center of the chamber.

Each of the side blanket modules is made up of thirteen sub-modules that vary in width and depth to accommodate the changing radius. Neutronics considerations set their minimum radial depth at 47 cm. Sub-modules consist of two, concentric rectangular tubes separated by a constant gap. As the shape of each sub-module changes, the hydraulic diameter remains constant. This insures sufficient velocity at the FW for good heat transfer at a reasonable pressure drop. Figure 3-4 provides an overall view of a sub-module and cross-sections at different elevations. The outer tube wall is made of 0.35-cm thick FS with a 0.1-cm thick diffusion bonded protective tungsten coating on the side facing the target. Liquid lithium enters each sub-module at the bottom, flowing at high velocity in the gap between the tubes to cool the FW. Vanes force the lithium to spiral upward and spend equal amounts of time on each side of the sub-module to even out the temperature. The lithium makes a U-turn at the top and travels back at very low velocity through the large internal channel, exiting out the bottom. Thus, the lithium is heated internally by absorbing neutrons, but poor heat transfer keeps the channel walls at a lower temperature.

More details are provided in the reference publication [Sviatoslavsky et al. (2005)]. Table 3-1 gives some relevant parameters from the design of this blanket.

The important information with regard to the potential for this conceptual design to drive a water-splitting process is the temperature range of the self-cooled blanket. The outlet

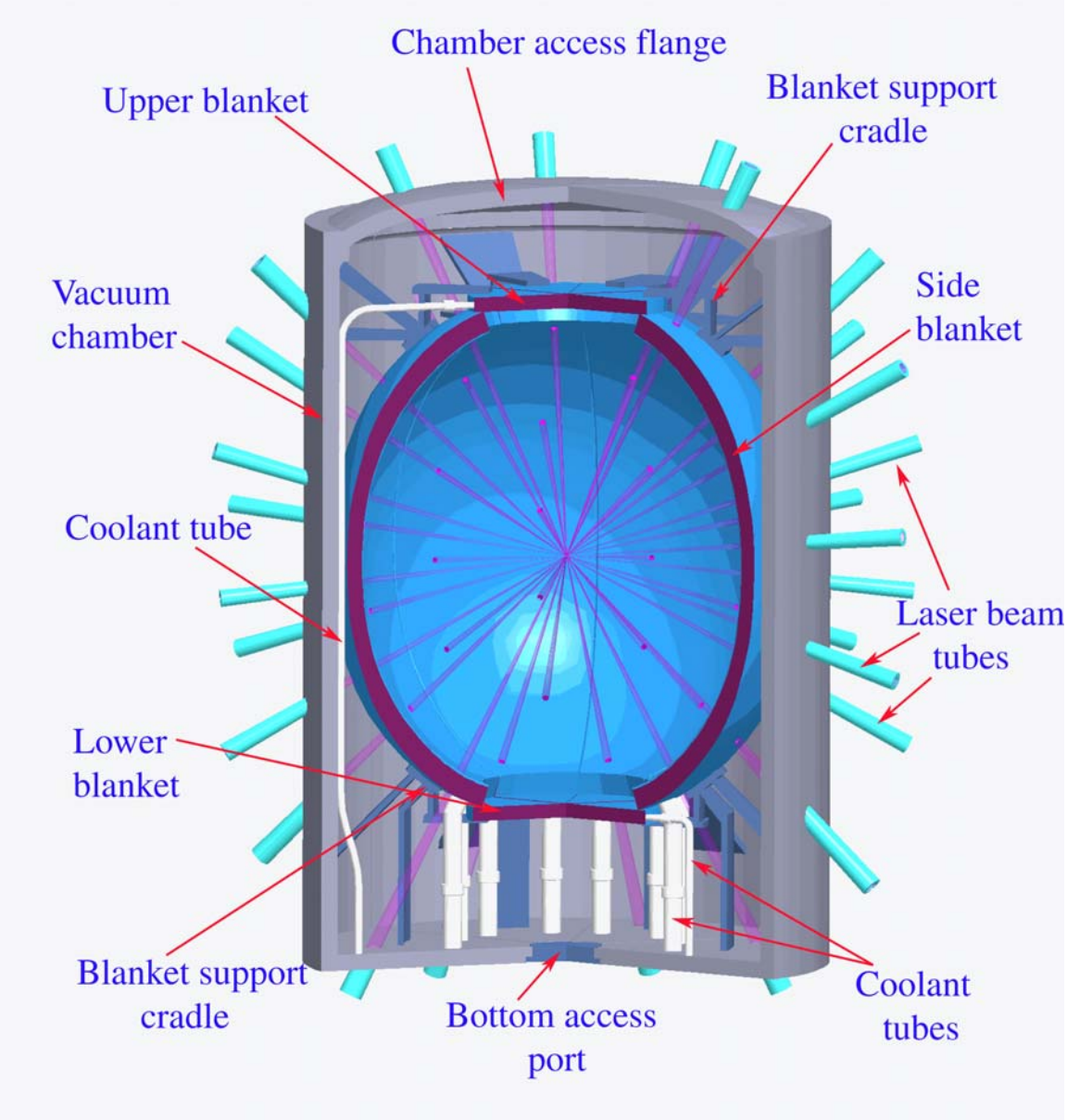

Figure 3-2 Cross-section of FS HAPL Chamber with Self-cooled Li Blanket
[Sviatoslavsky et al. (2005)]

Table 3-1 Selected Parameters for FS HAPL Chamber with Self-cooled Li Blanket
[Sviatoslavsky et al. (2005)]

Fusion Power (MW)	1,800
Total Thermal Power (MW)	2,103
FW Maximum Average Temperature (°C)	550
FS/Li Interface Maximum Temperature (°C)	600
Li Inlet Temperature (°C)	383
Li Outlet Temperature (°C)	650
Li Pressure Drop, MPa	< 0.5

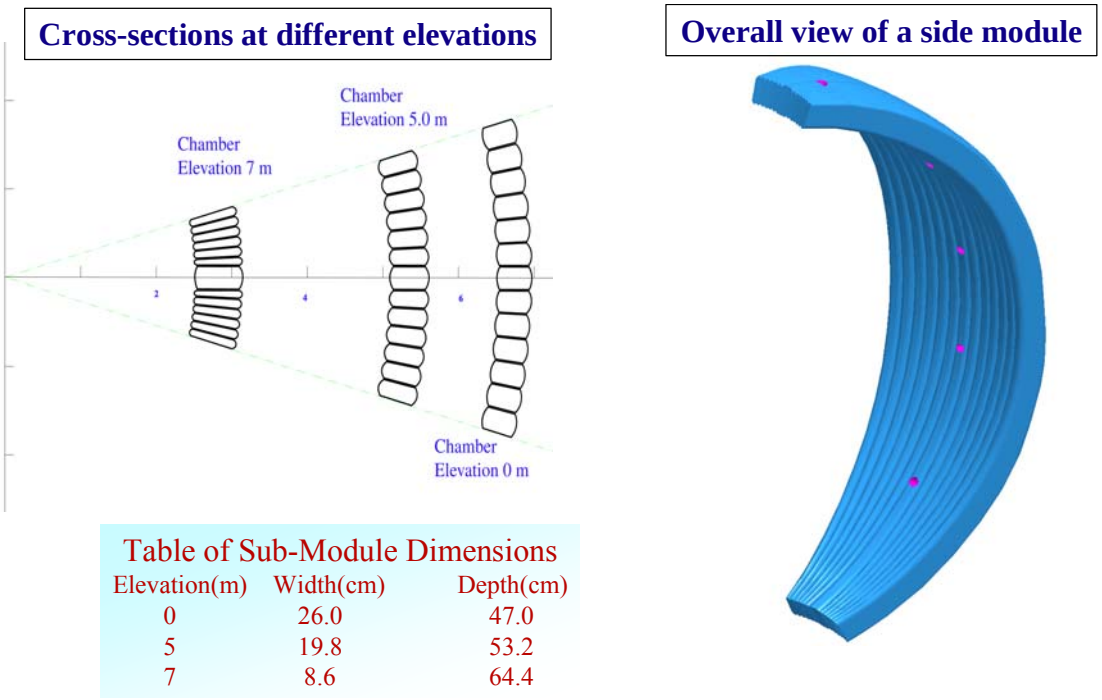

Table of Sub-Module Dimensions

Elevation(m)	Width(cm)	Depth(cm)
0	26.0	47.0
5	19.8	53.2
7	8.6	64.4

Figure 3-3 Side Blanket Module [Sviatoslavsky et al. (2005)]

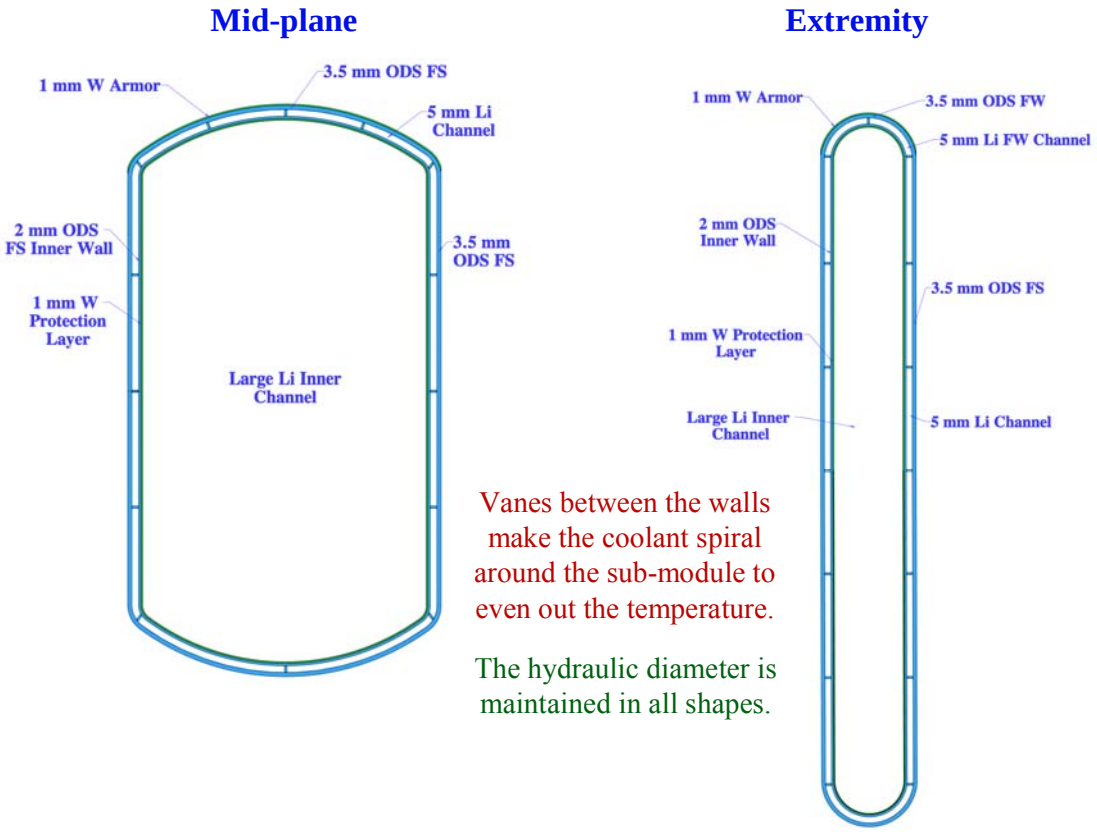

Figure 3-4 Cross-sections of a Side Blanket Sub-module [Sviatoslavsky et al. (2005)]

temperature was set at 650°C, based on F82H FS being used as the FW material of construction. F82H FS is constrained to a maximum average temperature of 550°C, while the maximum Li/FS interface temperature should be no more than 600°C. If the lithium outlet temperature were to be pushed higher, the maximum average temperature of the FW would begin to exceed the 550°C limit at 680°C.

Oxide Dispersion Stabilized (ODS) FS has a 150° higher maximum average temperature of 700°C. (The Li/FS interface temperature limit remains unchanged.) Using ODS FS in place of F82H would allow the outlet temperature of the self-cooled lithium blanket to be pushed as high as 800°C, above which the Li/FS interface temperature would begin to exceed 600°C.

Thus, for reaction chambers made from tungsten-armored FS and using a self-cooled Li blanket, 650°C appears to be a reasonable estimate of the outlet temperature, with a 220° temperature drop allowed for tritium recovery heat losses and hydrogen production heat requirements. The outlet temperature may have an upside of an additional 150°, depending on how much higher the maximum average temperature of the FW material can be pushed by using advanced FS formulations. Above an 800°C outlet temperature, the Li/FS interface condition becomes the limiting factor.

The second conceptual design, which uses magnetic diversion, is still being developed. However, enough information is available to determine the likely range of operating temperatures. A schematic diagram of the reaction chamber is given in Figure 3-5. The FW and blanket are shaped like opposing, stacked cones with a maximum radius of 6 m in the middle, tapering to points at top and bottom. Figure 3-6 provides a three-dimensional view of the chamber cross-section. Four externally-placed, ring-shaped coils apply a magnetic field that diverts ions emanating from the fusion reaction at the center to one of the armored ion dumps at the “equator” or “poles” of the chamber. Over 90% of the ion energy is dissipated in the resistive chamber walls, leaving less than 10% to be deposited with the ions on the sacrificial dump plates.

Eight modules comprise each of the two blanket mid-sections, extending from the base of the cone about three-quarters of the distance to the vertex, and subtending 45° of circumference. (See Figure 3-7.) Four smaller blanket modules cover each of the poles. The mid blanket modules are made up of ten sub-modules each that vary in width and depth to accommodate the changing radius. Sub-modules consist of two, concentric rectangular flow channels separated by a constant gap. As the shape of each sub-module changes, the hydraulic diameter remains constant. This insures sufficient velocity between the resistively heated channel walls for good heat transfer at a reasonable pressure drop. Figure 3-8 provides an overall view of a sub-module and cross-sections at different elevations. The channels are made from SiC_f/SiC, while the self-cooled blanket uses Pb-17Li. Liquid Pb-17Li enters each sub-module at its bottom, flowing at high velocity in the gap between the tubes to cool the walls. The liquid makes a U-turn at the top and travels back at very low velocity through the large internal channel, exiting out the bottom. Thus, the Pb-17Li is heated internally by neutron absorption, but poor heat transfer keeps that heat away from the channel walls.

More details are provided in the reference presentations [Sviatoslavsky (2006), Raffray (2006)].

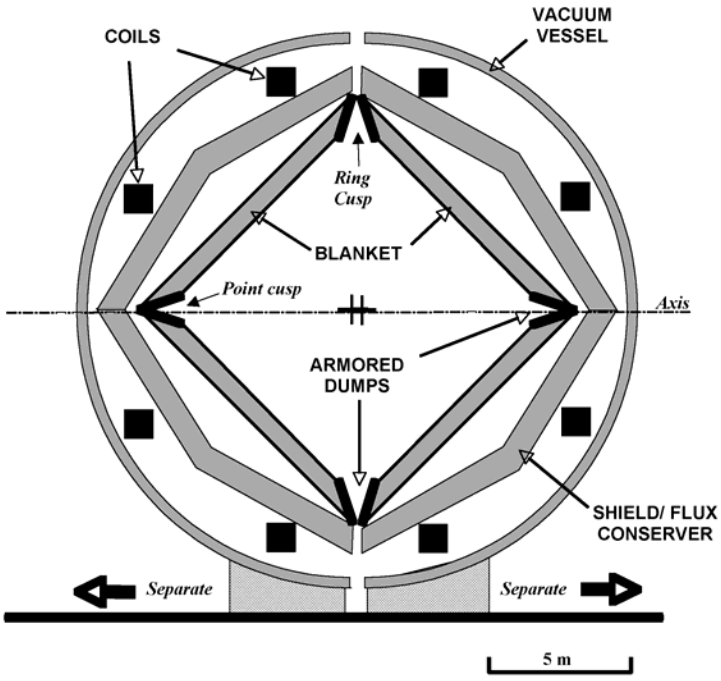

Figure 3-5 Cross-section of SiC_f/SiC HAPL Chamber with Magnetic Diversion and Self-cooled Pb-17Li Blanket [Raffray (2006)]

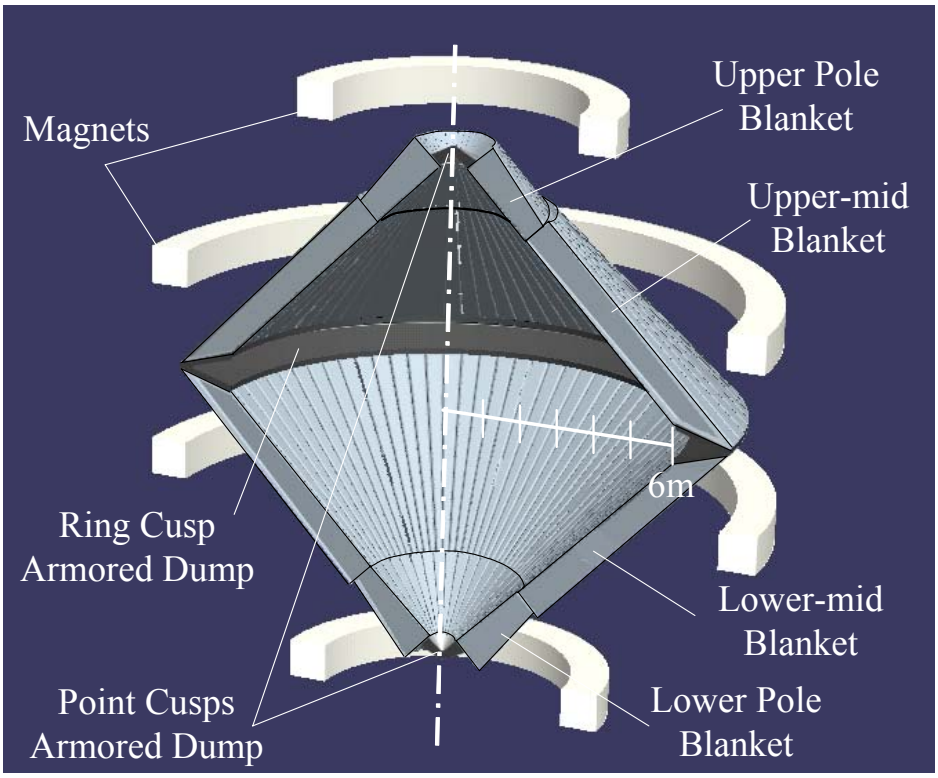

Figure 3-6 Chamber Cross-section with Magnetic Diversion [Sviatoslavsky (2006)]

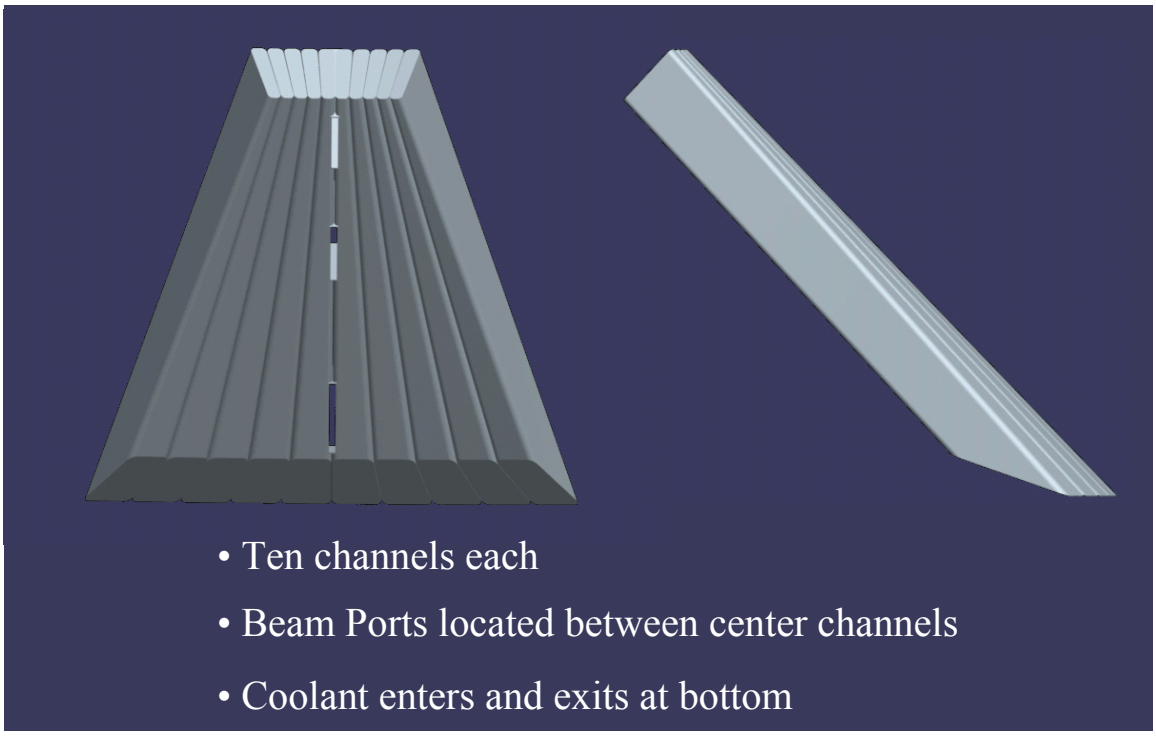

Figure 3-7 Mid Blanket Module [Sviatoslavsky (2006)]

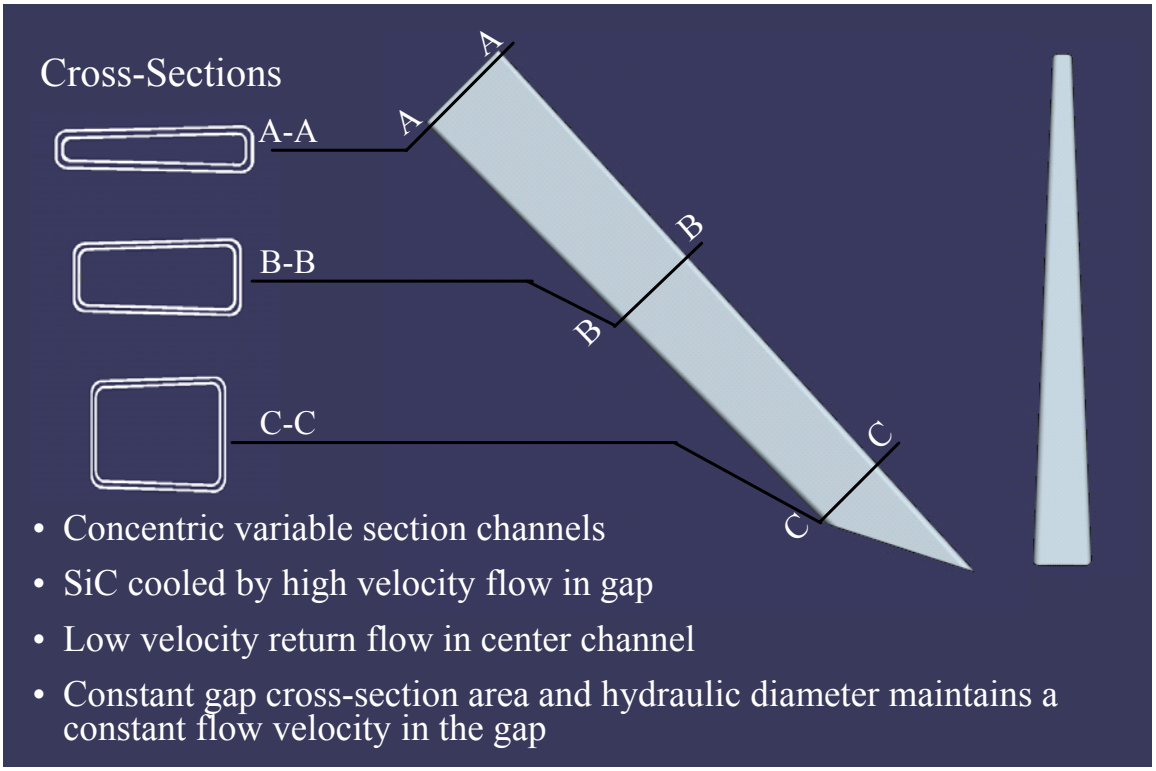

Figure 3-8 Mid Blanket Sub-module [Sviatoslavsky (2006)]

Preliminary calculations for a self-cooled Pb-17Li blanket with SiC_f/SiC reaction chamber walls showed that in order to keep the SiC_f/SiC maximum average temperature below 1,000°C, the outlet temperature could be no higher than 799°C. This would result in a maximum Pb-17Li/SiC interface temperature of 900°C. The Pb-17Li inlet temperature at these conditions would be 483°C and the pressure drop approximately 0.5 MPa. If the maximum wall material temperature limit was relaxed to 1,100°C, the coolant outlet temperature increased to 930°C, while the maximum coolant/material interface temperature grew to 950°C. The Pb-17Li inlet temperature at these conditions changed to 580°C while the pressure drop remained at roughly 0.5 MPa [Raffray (2006)].

Switching from Pb-17Li to a 34%-beryllium fluoride, 66%-lithium fluoride (Flibe) molten salt mixture as the self-cooled breeder blanket material appears to make the situation worse. The reason is that the relatively low Reynolds' Number and poor heat transfer properties calculated for Flibe result in less heat removal and higher pressure drop for a given SiC_f/SiC maximum temperature constraint. The 1,000°C maximum wall material temperature limit could only be met by keeping the Flibe outlet temperature no higher than 700°C. In that case, the maximum Flibe/SiC interface temperature would be 912°C, the Flibe inlet temperature would be 519°C, and the pressure drop about 1 MPa. Raising the SiC_f/SiC material temperature limit by 100° to 1,100°C increased the Flibe inlet temperature by only 90° to 790°C. The maximum Flibe/SiC interface temperature grew to 1,010°C, while the inlet temperature changed to 590°C. No discernible change in pressure drop was noted [Raffray (2006)].

Thus, for reaction chambers made from SiC_f/SiC and using a self-cooled Pb-17Li blanket with magnetic diversion, 930°C appears to be a reasonable estimate of the outlet temperature, allowing a 350° temperature drop for tritium recovery heat losses and hydrogen production heat requirements. The outlet temperature may have an upside, but there is not enough information available to make an evaluation.

3.4 Helium-cooled Blanket Concepts

One of the blanket concepts being evaluated for the ITER program DEMO fusion reactor is known as the Helium-Cooled Pebble Bed (HCPB) [Hermsmeyer (1999)]. A schematic of the HCPB concept, which is a typical helium-cooled blanket, is shown in Figure 3-9 [Diegele (2002)]. The FW and the bed structural components are made out of an advanced ODS FS. Alternating pebble beds of beryllium neutron multiplier and Li_4SiO_4 ceramic breeder are separated by cooling plates through which high pressure (8-MPa) helium is passed for heat removal. The helium is also used to cool the FW. Temperature limits on the FS structure restrict the coolant outlet temperature to no more than 500-550°C [Hermsmeyer (1999)]. Helium coolant inlet and outlet temperatures of 300°C and 500°C, respectively, have been reported for the DEMO blanket [Ihli (2006)]. Higher coolant temperatures could be achieved by making the structure out of SiC_f/SiC. While this specific blanket design is for a magnetic confinement fusion reactor, a similar design could probably be prepared for Laser IFE with comparable helium coolant operating conditions.

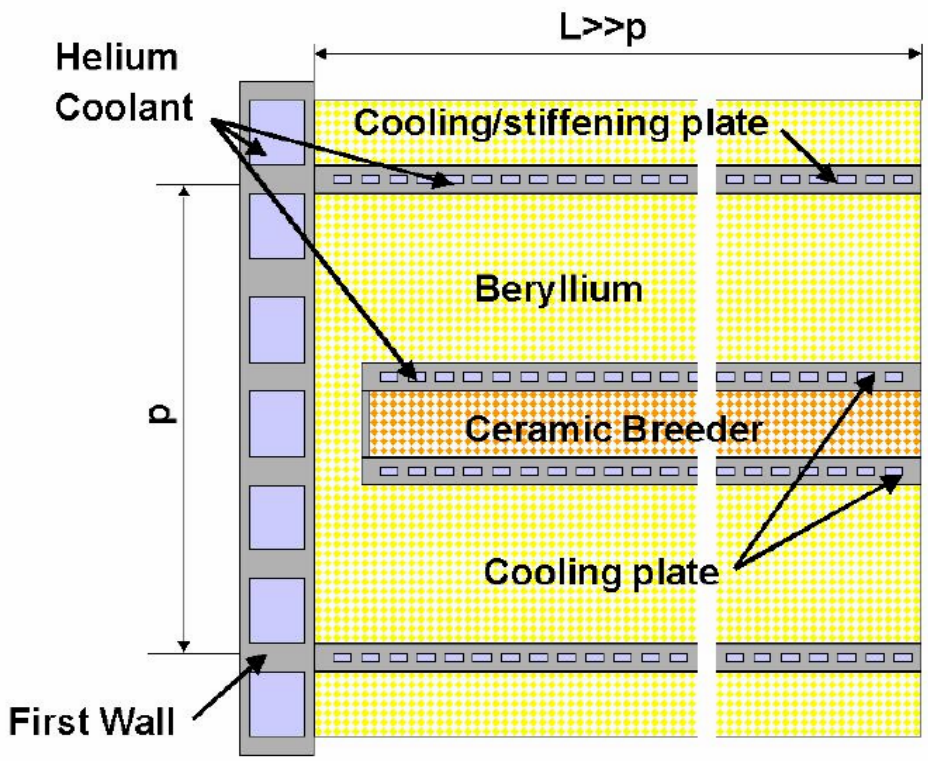

Figure 3-9 Helium-cooled Ceramic Breeder Concept (HCPB) [Diegele (2002)]

3.5 Dual-cooled Blanket Concepts

A variety of dual-cooled blanket concepts have been proposed for other fusion reactor development programs. The one depicted in Figure 3-10 was prepared for the ARIES magnetic confinement project [Tillack et al. (2003)]. As in the HCPB, the FW and the blanket structural components are made from FS and are cooled with high pressure helium. However, instead of a ceramic breeder blanket, this design uses self-cooled liquid Pb-17Li in the breeding zone. The liquid metal is confined to flow cells or channels that are lined with SiC_f/SiC for thermal insulation. (See Figure 3-11.) Since the Pb-17Li breeding blanket is internally heated by neutron absorption and capture, this allows it to attain temperatures that are significantly higher than the maximum operating temperature of the FS structure. However, the FS structure temperature limit still restricts the outlet temperature of the helium coolant.

One obvious drawback of this concept is its complexity. The FS and SiC_f/SiC concentric dual-flow channel sub-modules designs that have been proposed for HAPL so far look simple by comparison. Separate manifolds will be needed to handle the helium and Pb-17Li coolants. In addition, the breeder cells will need to be self-draining. Nevertheless, an adaptation of this concept should be feasible for HAPL. The outlet temperature for the Pb-17Li coolant will likely be comparable to that calculated for the coolant in the SiC_f/SiC HAPL chamber with magnetic diversion, but with an upside due to the absence of magnetic field-induced internal heating of the SiC and the additional structural cooling provided by the high pressure helium coolant.

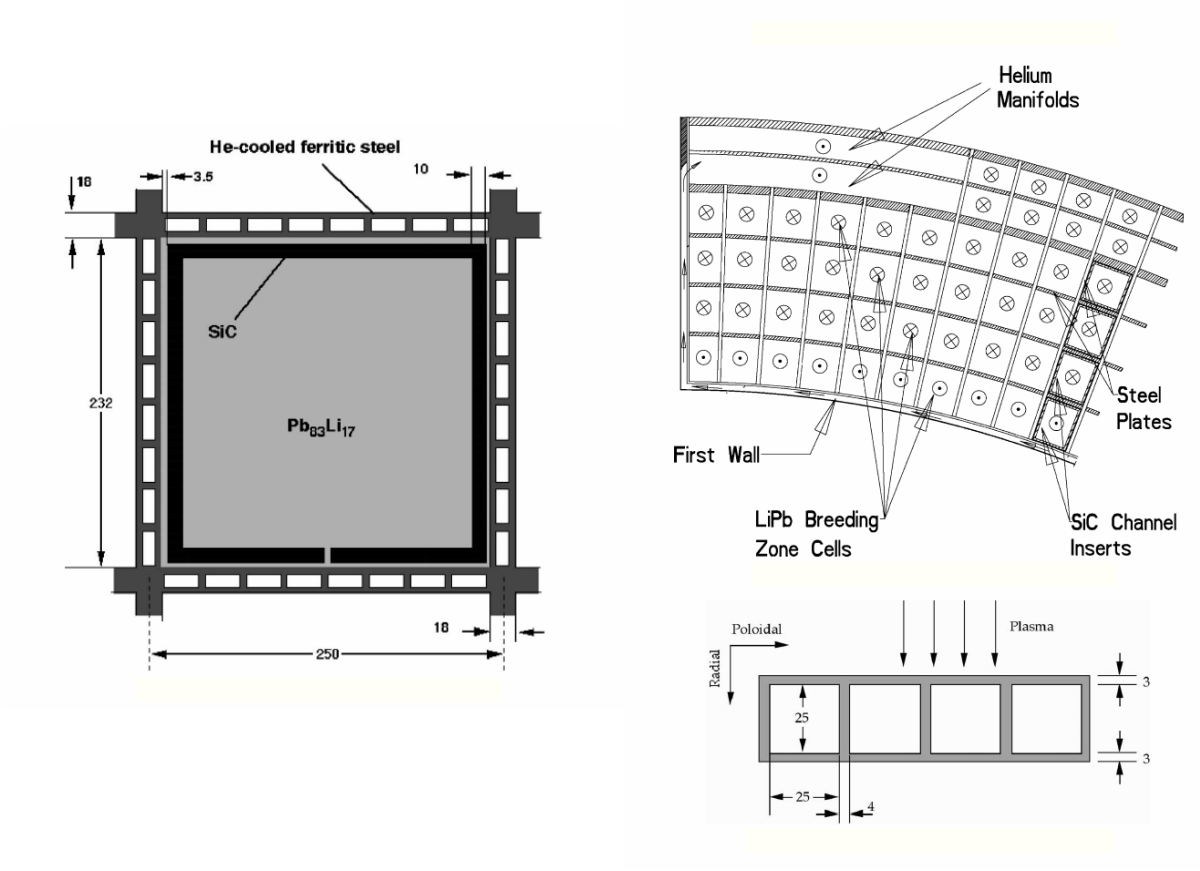

Figure 3-10 ARIES Dual-cooled Lead-lithium Blanket Concept [Tillack et al. (2003)]

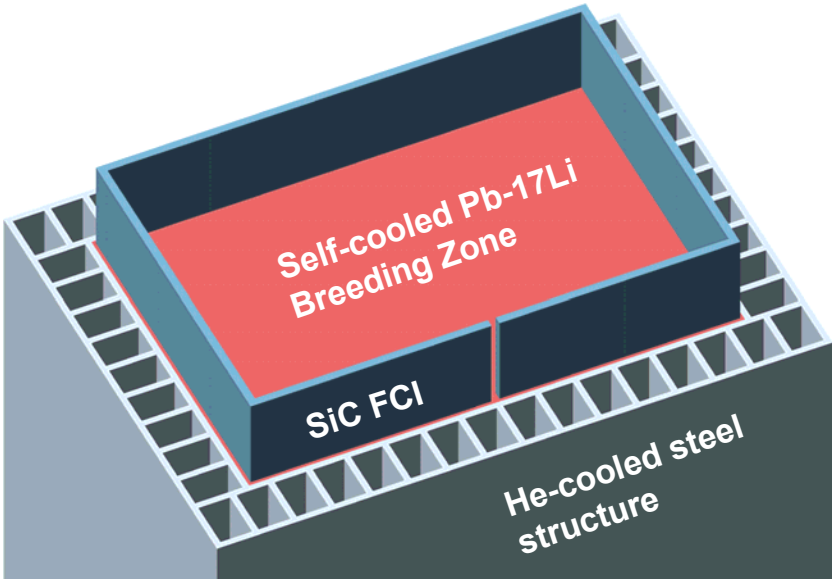

Figure 3-11 Typical Dual-cooled Lead-lithium Flow Cell [Morley et al. (2005)]

3.6 Advanced Blanket Concepts

The key characteristics of eight advanced FW/blanket concepts for magnetic confinement were recently tabulated [Wong et al. (2002)]. The results are summarized in Table 3-2 below. While these designs are not directly applicable to Laser IFE, they are included to show the kind of coolant conditions that might be possible with further development of FW/blanket concepts for HAPL. Note in particular that outlet temperatures as high as 1,100°C have been projected for helium (at 12 MPa pressure) and Pb-17Li. One concept uses lithium vapor as coolant to achieve a projected outlet temperature of 1200°C (at 0.037 MPa pressure).

Table 3-2 Key design parameters of eight advanced FW/blanket designs [Wong et al. (2002)]

	1	2	3	4	5	6	7	8
	A-SSTR-2	A-HCPB	TAURO	ARIES-AT[1]	V/Li/He	W/Li/He	EVOLVE	FFHR-2
Application	Tokamak	Tokamak	Tokamak	Tokamak	Tokamak	Tokamak	Tokamak	Stellerator
P_{fusion}, GW	4	4.5	3	1.7	1.9	3.5	3.5	1
FW heat flux, MW/m^2	1.4 (ave.)	0.6 (peak)	0.5 (ave) 0.69(peak)	0.26 (ave) 0.34(peak)	0.34	2 (peak)	2 (peak)	0.09
Neutron wall loading, MW/m^2	6 (ave.)	2.76(ave.) 3.5 (peak)	2 2.8 (peak)	3.2 (ave)	2.9 (ave)	7(peak)	10 (peak)	1.7
Structural material	SiC_f/SiC composite	SiC_f/SiC	SiC_f/SiC composite	SiC_f/SiC composite	V-4Cr-4Ti	W-alloy	W-alloy	V-4Cr-4Ti
FW thickness, mm	4–6	3	6	4 +1(armor)	3	3	3	5
Structural material T_{max}-allowed, °C	1100	1300	1300	1000	700	1400	1400	750
FW material, K_{th}, W/m-K	10–50	15	15	20	35	85 @1400 K	85 @ 1400 K	35
Tritium breeder (neutron multiplier)	Li_2TiO_3 (Be)	Li_4SiO_4 (Be)	Pb-17Li (none)	Pb-17Li (none)	Li (none)	Li (none)	Li (none)	Flibe (Be)
Fuel form	Pebbles	Pebbles	Liquid	Liquid	Liquid	Liquid	Liquid	Liquid
Coolant (Pressure, MPa)	He (10)	He (8)	Pb-17Li (1.5)	Pb-17Li (1)	He (18)	He (12)	Vaporized Li (0.037)	Flibe (0.6)
Tritium breeding ratio (Li-6 enrichment)	1.37 (local) (natural)	1.09 "3-D" (optimized)	1.37 (local) (90%)	1.1 "3-D" (natural)	1.4 (local) (natural)	1.43 (local) (35%)	1.33 (local) (natural)	1.4 (local) (50%)
Coolant T_{in}, °C	600	350	650	654	400	800	1100	450
Coolant T_{out}, °C	900	700	860	1100	650	1100	1200	550
Power conversion cycle	CCGT[2]	CCGT[2]	CCGT[2]	CCGT[2]	CCGT[2]	CCGT[2]	CCGT[2]	CCGT[2]
η_{th}, %	51	44.8	>47	58.5	46	57.5	58	45

[1]For ARIES-AT the surface heat flux used for temperature and stress calculation was 0.7 MW/m^2.

[2]Closed Cycle Gas Turbine

3.7 Blanket Concepts Evaluated

For the purpose of this white paper, the following cases will be evaluated with respect to their potential to serve as heat sources for water-splitting processes to produce hydrogen:

1. Liquid lithium self-cooled blanket with tungsten-armored FS FW chamber [Sviatoslavsky et al. (2005)]; T_{outlet} = 650°C, T_{intlet} = 383°C, P = 0.5 MPa.
2. Liquid lithium self-cooled blanket with tungsten-armored ODS FS FW chamber [Sviatoslavsky et al. (2005)]; T_{outlet} = 800°C, T_{intlet} = 533°C, P = 0.5 MPa.
3. Liquid Pb-17Li self-cooled blanket with SiC_f/SiC chamber and magnetic diversion, 1,000°C material temperature limit [Raffray (2006)]; T_{outlet} = 799°C, T_{intlet} = 483°C, P = 0.5 MPa.
4. Liquid Pb-17Li self-cooled blanket with SiC_f/SiC chamber and magnetic diversion, 1,100°C material temperature limit [Raffray (2006)]; T_{outlet} = 930°C, T_{intlet} = 580°C, P = 0.5 MPa.
5. Adaptation of Advanced HCPB blanket with SiC_f/SiC structural material [Wong et al. (2002)]; T_{outlet} = 700°C, T_{intlet} = 350°C, P = 8 MPa.
6. Adaptation of Pb-17Li self-cooled ARIES-AT blanket with SiC_f/SiC structural material [Wong et al. (2002)]; T_{outlet} = 1,100°C, T_{intlet} = 800°C, P = 1 MPa.

The first four cases were taken from conceptual designs that had been specifically prepared for the HAPL program, while the last two are advanced blanket concepts developed for magnetic confinement devices. Cases 5 and 6 are intended to represent the temperature limits to which helium-cooled and self-cooled blankets for HAPL could possibly be extended. (Preliminary attempts to increase the maximum temperature of the Pb-17Li coolant in the SiC_f/SiC chamber with magnetic diversion by optimizing the first wall while maintaining stresses at an acceptable level and increasing the size of the chamber actually resulted in a Pb-17Li outlet temperature of around 1100°C [Raffray email (2006)].) The HCPB [Hermsmeyer (1999)] and other helium-cooled concepts using FS structures were not considered because the 500-550°C coolant outlet temperatures to which they are restricted are too low for efficient water-splitting processes currently under development. This is discussed further in Section 5. Dual-cooled concepts were likewise not explicitly included because the ranges of coolant temperatures involved should be includes in the six cases above.

4.0 THEORETICAL EFFICIENCY LIMITS

When considering the cost to build a hypothetical Laser IFE hydrogen production plant, it is reasonable to assume that by far the most expensive component will be the fusion heat source. Consequently, the net thermal efficiency of the hydrogen production process is probably the single most important factor in determining whether Laser IFE can be used as a practical energy source for making hydrogen by splitting water. The more hydrogen that can be made per unit of heat output from a given fusion energy source, the lower the unit cost of hydrogen production. Net thermal efficiency, in turn, depends on the temperature range over which the heat from the fusion reaction is transferred to the hydrogen production process.

4.1 Ideal Net Thermal Efficiency for a Water-splitting Process

For a synthetic fuel process, one possible definition of net thermal efficiency compares the enthalpy difference between the synthetic fuel product and the process feedstock with the total amount of heat required from the primary energy source to effect the conversion,

$$\eta_p = \frac{\Delta \dot{H}}{\dot{Q}_T}. \tag{1}$$

Here $\Delta \dot{H}$ is the enthalpy change between the end product and the starting materials, $\dot{Q}_T$ is the total heat requirement from the primary energy source, and η_p is the process-based net thermal efficiency. For the special case of water-splitting, the enthalpy change may be calculated from the molar flow rate of water processed, $\dot{n}_{H_2O}$, and the specific molar enthalpies of water, hydrogen, and oxygen, h_{H_2O}, h_{H_2}, and h_{O_2},

$$\Delta \dot{H}_{H_2O} = \dot{n}_{H_2O}(h_{H_2} + \tfrac{1}{2}h_{O_2} - h_{H_2O}). \tag{2}$$

Note that if liquid water is fed to the process and gaseous hydrogen and oxygen products are withdrawn at typical ambient conditions (25°C and 1 bar pressure), the term inside the parentheses is simply the molar higher heating value (HHV) of hydrogen fuel, ΔH_{HHV}, equal to 285.8 kJ/mol H_2.

Consider the simplified water-splitting hydrogen production process illustrated in Figure 4-1 below. Energy is provided to the process by heat transfer from a hot fluid that enters across the process boundary at temperature T_1 and pressure P_1, and exits across the process boundary at temperature T_2 and pressure P_2. This fluid could be the self-cooling breeder blanket from a Laser IFE device transferring heat recovered from the fusion reaction. Applying the definition of net thermal efficiency in equation (1) to this process implicitly assumes that no useful work is being performed on the process from any external source (i.e. any mechanical or electrical work required by the process is internally generated) and that the only export of energy is in the form of hydrogen fuel.

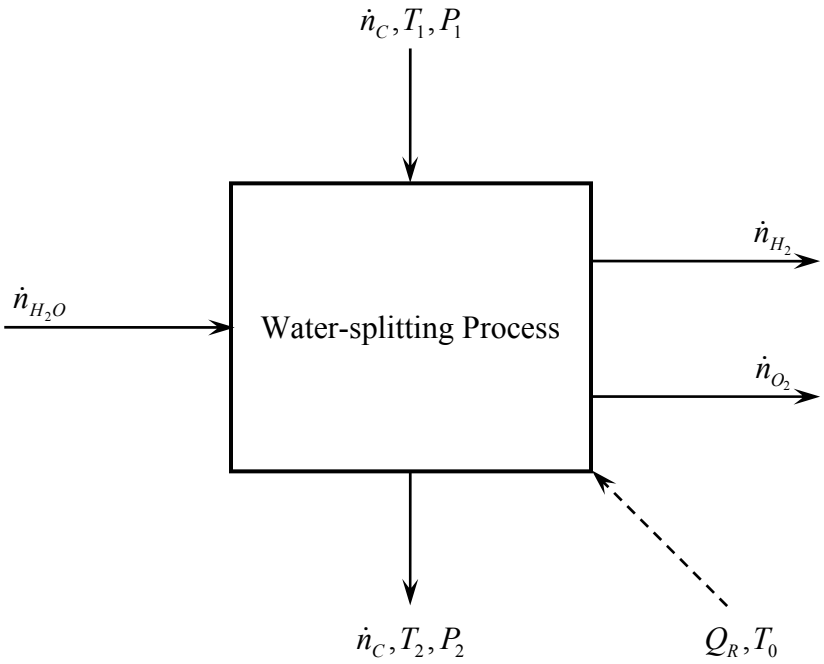

Figure 4-1 Simplified Water-splitting Hydrogen Production Process

Knoche and Funk (1977) have shown that the limiting or ideal thermal efficiency for this situation, $\eta_{p,id}$, is given by

$$\eta_{p,id} = \frac{T_m - T_0}{T_m} \frac{\Delta \dot{H}}{\Delta \dot{H} - T_0 \Delta \dot{S}}, \tag{3}$$

where T_m is the thermodynamic mean temperature of the coolant, T_0 is the temperature of the surroundings, and $\Delta \dot{S}$ is the entropy change between the hydrogen and oxygen product streams and the water feed stream. No real water-splitting process can operate with an efficiency higher than $\eta_{p,id}$, since that represents the ideal limit in which all of the process operations are carried out in completely reversible fashion.

The thermodynamic mean temperature of the coolant is defined as

$$T_m = \frac{h_{C,1} - h_{C,2}}{s_{C,1} - s_{C,2}}, \tag{4}$$

where $h_{C,1}$ and $s_{C,1}$ are the specific enthalpy and entropy of the hot coolant entering the process, and $h_{C,2}$ and $s_{C,2}$ are the corresponding values for cold coolant leaving the process. If the coolant is a liquid metal or salt, as would be the case for a self-cooling breeder blanket, the molar heat capacity will not vary significantly and it may also be considered incompressible. In that case, the thermodynamic mean temperature may be closely approximated by the logarithmic mean,

$$T_m = \frac{T_1 - T_2}{\ln\left(\frac{T_1}{T_2}\right)}. \tag{5}$$

Factoring out and canceling the molar flow rate of water processed ($\dot{n}_{H_2O}$) in the numerator and denominator of equation (3) and substituting the log-mean coolant temperature for T_m, equation (3) simplifies to

$$\eta_{p,id} = 1 - \frac{T_0}{T_1 - T_2}\ln\left(\frac{T_1}{T_2}\right)\frac{\Delta H}{\Delta H - T_0 \Delta S}. \tag{6}$$

Furthermore, as noted above, if liquid water is fed to the process and gaseous hydrogen and oxygen products are withdrawn at typical ambient conditions (25°C and 1 bar pressure), $\Delta H = -\Delta H^o_{f,H_2O} = 285.8$ kJ/mol H_2, $\Delta S = -\Delta S^o_{f,H_2O} = 0.16334$ kJ/K-mol H_2, $T_0 = 298.15$K, and equation 6 becomes

$$\eta_{p,id} = 1.205 \times \left[1 - \frac{T_0}{T_1 - T_2}\ln\left(\frac{T_1}{T_2}\right)\right]. \tag{7}$$

This expression provides an upper limit for the efficiency of a water-splitting process that is driven by heat transferred from a recirculating, incompressible, high-temperature fluid that has a constant specific heat. Real processes may operate with net thermal efficiencies as high as 60-70% of ideal if properly designed to maximize energy utilization, but most fall short.

4.2 Net Thermal Efficiency Estimates for HAPL

Ideal net thermal efficiencies were calculated for the six blanket concepts listed in Section 3.7 using equation (7) and tabulated in Table 4-1 below.

Table 4-1 Net Thermal Efficiency Estimates for HAPL Blanket Concepts

Case No.	T_1, °C	T_2, °C	$\eta_{p,id}$ *	$\eta_{p,max}$ *
1. Li / FS	383	650	0.746	0.481
2. Li / ODS FS	533	800	0.820	0.529
3. Pb-17Li / SiC_f/SiC (1,000°C)	483	799	0.808	0.522
4. Pb-17Li / SiC_f/SiC (1,100°C)	580	930	0.852	0.550
5. He / SiC_f/SiC A-HCPB	350	700	0.747	0.482
6. Pb-17Li / SiC_f/SiC ARIES-AT	800	1,100	0.910	0.587

* assumes $T_0 = 25$°C

The fourth column lists the ideal efficiency limits, $\eta_{p,id}$, which represent the efficiencies that would be obtained for a reversible water-splitting process connected to each of the given blanket coolants. These need to be converted to real water-splitting process efficiencies to be useful. The last column lists the maximum expected efficiencies for real processes as discussed below.

As noted in Section 1.2, DOE's Office of Nuclear Energy, Science & Technology (DOE-NE) is sponsoring the development of water-splitting technologies for use with advanced fission reactors through the NHI. The high temperature heat input to these water-splitting processes is within the range of temperatures being considered for HAPL, so they can serve as a reference point. For example, General Atomics' (GA's) Hydrogen Modular Helium Reactor, the H2-MHR, is one of the designs being used as the basis for NHI development. The H2-MHR's primary coolant is helium gas at 7 MPa with an outlet temperature of 950°C and an inlet temperature of 590°C. This is close to the temperature range of blanket Case No. 4.

Most of the NHI's resources are being devoted to the parallel development of three different water-splitting technologies: High Temperature Electrolysis (HTE), the Sulfur-Iodine cycle (SI), and the Hybrid Sulfur (HyS) cycle. Each of these processes is discussed in detail in Section 5. Performance claims for these processes when coupled to an H2-MHR heat source are similar and fall in the 45-55% net thermal efficiency range (HHV basis), depending on flowsheet configuration and other factors. Therefore, a reasonable estimate of the maximum net thermal efficiency that might be obtained with a properly designed water-splitting process coupled to a Laser IFE heat source using blanket Case No. 4 would be 55%, or 0.550.

Accepting 55% as the maximum efficiency estimate for blanket Case No. 4, estimates of the potential water-splitting net thermal efficiency for the other blanket cases can be obtained by extrapolating in proportion to the ideal efficiency. These estimates are listed in the last column in Table 4-1, under the heading $\eta_{p,max}$.

Not surprisingly, the maximum water-splitting efficiency estimates are comparable to and generally higher than the electric power conversion efficiency estimates that have been calculated for these blanket cases. That comparison can be seen in Table 4-2. The values of the power conversion efficiency, η_e, for each blanket case were calculated for Brayton closed cycle gas turbine generators specifically optimized for that blanket, as reported in the references cited.

Since the simplest and most established means to split water is through conventional low temperature electrolysis, which has a conversion efficiency of 75-85% (H_2 HHV/electric power input), this should be considered as a baseline for developing high temperature water-splitting technologies for use with fusion heat sources. (In fact, electrolysis is the only other water-splitting option that can use fusion as the primary energy source.) Predicted electric power conversion efficiency has been shown to be less than or equal to the estimated maximum hydrogen production efficiency for a fusion heat source. Low temperature electrolysis using nuclear fusion power compounds power conversion losses with electrolysis conversion losses, since the net thermal efficiency for hydrogen production is the product of the electric generating efficiency and the electrolysis efficiency. Consequently, if fusion heat is the primary energy source, hydrogen production via electrolysis should be significantly

less thermally efficient than high temperature water splitting. Values of the effective net thermal efficiency for hydrogen production via conventional electrolysis using fusion electric power, $\eta_{p,\,elec}$, are listed in the last column in Table 4-2. The high temperature water splitting efficiencies are 24-50% more efficient than the electric power/electrolysis efficiencies for the various blanket concepts studied.

Table 4-2 Comparison between Net Thermal Efficiencies for High Temperature Water-splitting Versus Electrolysis

Case No.	$\eta_{p,\,max}$	η_{e}	$\eta_{p,\,elec}$ *
1. Li / FS	0.481	0.40[a]	0.32
2. Li / ODS FS	0.529	0.47[a]	0.38
3. Pb-17Li / SiC_f/SiC (1,000°C)	0.522	0.50[b]	0.40
4. Pb-17Li / SiC_f/SiC (1,100°C)	0.550	0.55[b]	0.44
5. He / SiC_f/SiC A-HCPB	0.482	0.45[c]	0.36
6. Pb-17Li / SiC_f/SiC ARIES-AT	0.587	0.585[d]	0.468

* assumes electrolysis efficiency (H_2 HHV/power input) = 0.8

a [Sviatoslavsky et al. (2005)]

b [Raffray (2006)]

c [Boccaccini et al. (2000)]

d [Raffray et al. (2006)]

5.0 WATER-SPLITTING OPTIONS FOR HAPL

The thermodynamics of the water-splitting reaction,

$$H_2O(g) \rightarrow H_2(g) + \tfrac{1}{2}O_2(g),$$

are summarized in the table below:

Table 5-1 Thermodynamics of the Water-splitting Reaction

Temperature, K	Temperature, °C	$\Delta H°$, kJ/mol*	$\Delta G°$, kJ/mol*
298	25	241.8	228.5
500	227	243.8	219.1
1,000	727	247.9	192.6
1,500	1,227	250.3	164.4
2,000	1,727	251.6	135.5
2,500	2,227	252.4	106.4
3,000	2,727	253.0	77.2
3,500	3,227	253.7	47.8
4,000	3,727	254.5	18.3

* standard state pressure = 1 bar

Large positive values for the enthalpy change, $\Delta H°$, indicate that the reaction is strongly endothermic – not at all surprising since the reverse reaction is the combustion of hydrogen gas. Higher temperatures do not change the value of $\Delta H°$ significantly (it actually increases slightly), so raising the temperature does not reduce the net total energy requirement. However, the free energy change, $\Delta G°$, decreases steadily with increasing temperature, becoming negative above 4,000°C.

If the free energy change of a process is greater than zero, the process is not favored thermodynamically and can only proceed if work is performed on it. Thus, $\Delta G°$ is a measure of how much work must be performed to achieve the desired change. At low temperatures, most of the energy requirement for water-splitting has to be provided in the form of work, e.g. by flowing current against a potential difference in an electrochemical cell:

$H_2O(l) \rightarrow \tfrac{1}{2}O_2(g) + 2H^+(aq) + 2e^-$	anode reaction
$2H^+(aq) + 2e^- \rightarrow H_2(g)$	cathode reaction
$H_2O(l) \rightarrow H_2(g) + \tfrac{1}{2}O_2(g)$	net reaction

These reactions, in fact, describe the electrolysis of water, for which the standard cell potential is $E° = -1.23$ V at 25°C, calculated from the standard free energy change for the decomposition of liquid water, $\Delta G° = 237.1$ kJ/mol, via

$$E^o = \frac{-\Delta G}{zF} = \frac{-(237.1\ kJ/mol)(1000\ J/kJ)}{(2\ eq/mol)(96{,}485.3\text{C/eq})} = -1.23\,\text{V}.$$

Here z is the number of electron equivalents transferred per mole of reaction and F is Faraday's constant.

Since heat can not be used directly to split water at low temperatures, but must first be converted to electrochemical work, this implies an inherent conversion loss or inefficiency. That is one of the reasons why the effective net thermal efficiencies for hydrogen production via electrolysis in Table 4-2 were lower than the estimated efficiencies for high temperature water-splitting. The other reason has to do with the fact that the free energy change for splitting water decreases steadily with increasing temperature. Thus, at higher temperatures, an ever smaller fraction of the energy requirement must be in the form of work instead of heat, conversion losses are reduced, and efficiency is increased.

Three alternatives to low temperature electrolysis become available as the temperature at which the water-splitting takes place is increased:

- direct thermolysis, or thermal decomposition
- high temperature steam electrolysis (HTE)
- thermochemical water-splitting

Thermolysis can be dismissed immediately from any further consideration due to the extreme temperature requirements (4000 °C). (Other considerations, such as materials of construction and the need for separation to prevent the reverse reaction, also limit consideration of direct thermolysis). The highest temperature being considered here is 1,100°C, for which the water-splitting reaction free energy change is approximately 175 kJ/mol (estimated from Table 5-1). Therefore, fusion heat from a self-cooled blanket alone can not be used to perform water thermolysis in any practical way. However, thermochemical cycles and HTE are both viable options for the efficient splitting of water at high temperatures using Laser IFE.

5.1 Thermochemical Cycles

A thermochemical water-splitting cycle is a cyclic chemical process that uses a series of chemical reactions that combine to split water. All intermediate species are regenerated, so that the only feed is water and the only products are hydrogen and oxygen. The challenge for a practical cycle is in finding a series of reactions for which the free energy changes are less than or equal to zero. True thermochemical cycles use heat flows alone to drive the chemical reactions. This requires that all of the reactions that comprise the cycle have free energy changes that are less than or equal to zero. (Small positive free energy changes will work too.) Hybrid cycles use a combination of both heat and electrical work to drive the process, implying that at least one of the reactions has a significantly positive free energy change. At least 115 different cycles have been proposed in the open literature [Brown et al. (2000)].

Of the many cycles that have been conceived, two stand out as the most likely candidates for the range of temperatures that Laser IFE blanket coolants afford: the SI and the HyS cycles.

These are also the two cycles that are the current focus of DOE-NE's thermochemical development efforts under the NHI, as well as the focus of international research and development on hydrogen production from advanced nuclear heat sources.

5.1.1 Sulfur-Iodine Cycle

The SI cycle, depicted schematically in Figure 5-1 below, consists of three chemical reactions, coupled in two oxidation-reduction loops. The process involves thermal decomposition of sulfuric acid, or H_2SO_4 (top) and hydrogen iodide, or HI (bottom), followed by regeneration of both reagents using the exothermic Bunsen reaction (middle). Heat must be supplied at temperatures greater than 800°C to concentrate and decompose H_2SO_4. The exothermic Bunsen reaction is performed at temperatures below 120° C and releases waste heat to the environment. Hydrogen is generated by the decomposition of HI, using heat at temperatures greater than 300° C. The sum of these three reactions is the splitting of one mole of water (H_2O) into one mole of hydrogen (H_2) and one-half mole of oxygen (O_2).

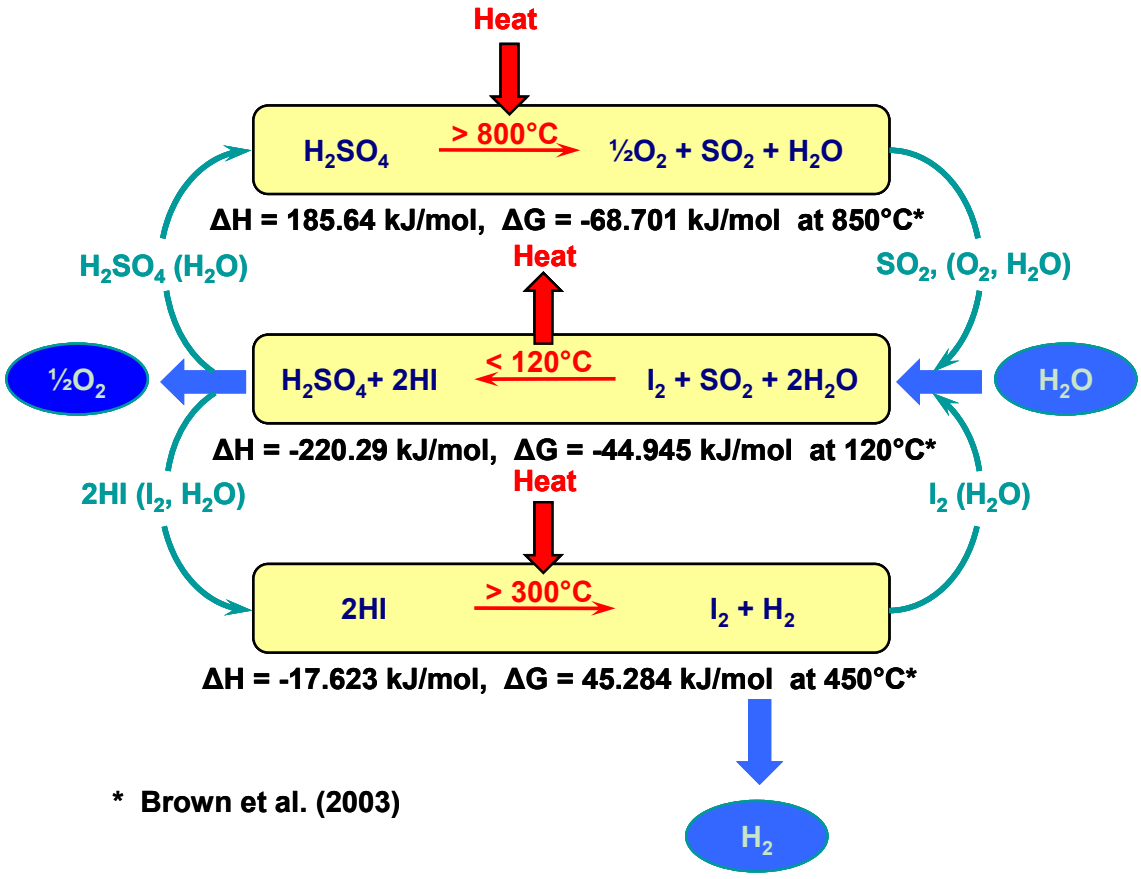

Figure 5-1 Sulfur-Iodine Cycle Schematic Diagram

Thermodynamics suggests that the very endothermic H_2SO_4 decomposition and very exothermic Bunsen reactions should both proceed to high levels of conversion since the free energy change of the reactions is significantly less than zero. The same is not true for the

decomposition of HI, which has a free energy change that is substantially greater than zero. However, that reaction results in a two-fold reduction in the number of moles of gaseous species ($2\ HI(g) \rightarrow H_2(g) + I_2(l)$), since iodine (I_2) will go primarily into the liquid phase. Therefore, the reaction can be "pushed" to the right at high pressures with removal of the H_2 product (which is easily separated from HI on the basis of relative volatility).

The SI cycle was first proposed by General Atomics in the 1970s, during the rush to develop alternative energy sources following the oil embargo crisis of 1973-74. It was initially rejected because the H_2SO_4 and HI products of the Bunsen reaction could not be separated by conventional distillation. However, the discovery that using an excess of molten I_2 would cause them to separate into two immiscible liquid phases led to development of a complete process concept [Norman et al. (1978)]. A simplified block flowsheet based on this concept and adapted to fit blanket Case No. 4 is shown in Figure 5-2 below.

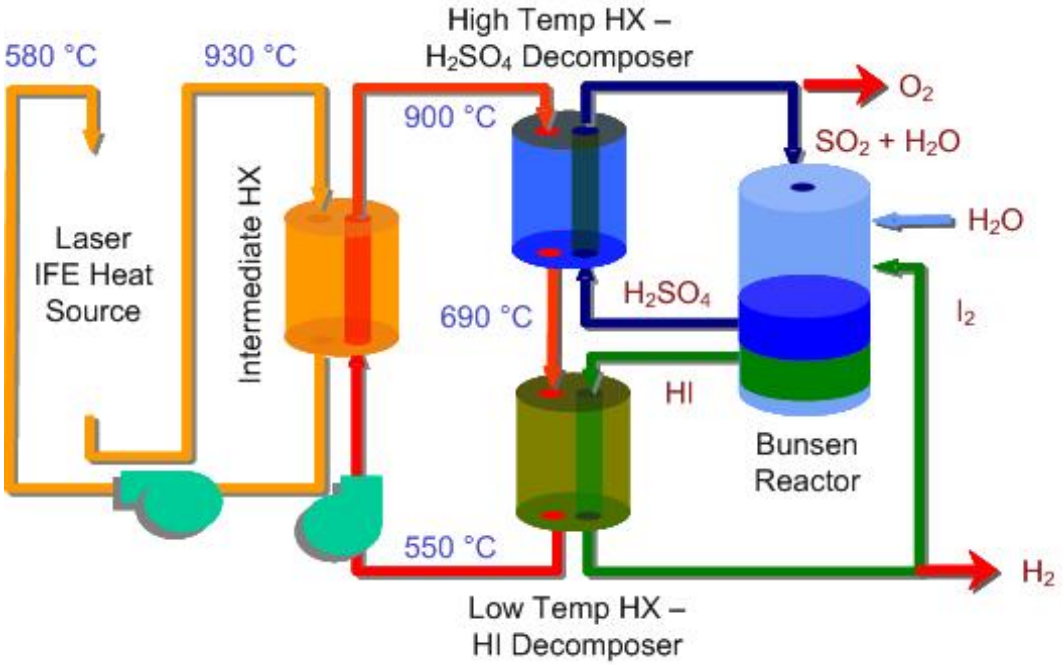

Figure 5-2 Simplified Flowsheet of Laser IFE-driven SI Cycle Process [adapted from Summers (2006)]

According to this scenario, the self-cooled Pb-17Li blanket would transfer its heat to a secondary coolant loop in an intermediate heat exchanger (IHX). The secondary heat transfer fluid could be pressurized helium or a molten salt mixture. A 30-degree temperature difference is shown across the IHX, but the actual value would depend on the transport properties of the fluid and on the design of the IHX. In any event, the secondary coolant loop would heat the H_2SO_4 decomposition reaction to a temperature as high as 850 to 875°C, more than enough to achieve satisfactory conversion. All of the heat needed to concentrate and vaporize the H_2SO_4, as well as to drive the decomposition reaction for HI, would be supplied by the secondary coolant loop, either by direct heat exchange, or indirectly by interchange with hotter process streams. This is identical to the approach used for the recent conceptual design of a H_2 production facility coupled to an advanced nuclear fission heat

source prepared under DOE-NE's Nuclear Energy Research Initiative (NERI) [Summers (2006)].

The SI cycle has been extensively studied by investigators in the US, Europe, Japan and other countries around the world. Of all the thermochemical cycles, it has enjoyed the most research and development (R&D) effort because it is an all-fluids process that is relatively simple and amenable to conventional scale-up from the laboratory bench. (Most other cycles involve solid species, more reactions, and/or one or more electrochemical steps.) While the process is well-defined in general, considerable uncertainty remains about how to accomplish the HI decomposition reaction.

Early versions of the SI cycle were based on the assumption that it was necessary to separate HI from the heavy I_2-HI-H_2O phase obtained in the Bunsen reaction before decomposing it in the vapor phase. This culminated in a flowsheet that used phosphoric acid extraction to obtain pure HI, subsequently decomposed in the vapor phase over an activated carbon catalyst [Besenbruch (1982)]. However, the estimated capital cost for this process was high. The phosphoric acid concentration step alone accounted for over 40% of the capital cost for the entire process [Brown et al. (2003)]. The reason for this was that three-stage vapor recompression was needed to bolster the thermal efficiency of phosphoric acid evaporation [Norman et al. (1982)]. The net thermal efficiency of the overall flowsheet was estimated at 47% (HHV basis), the highest value achieved for a thermochemical H_2 cycle at that time [Brown et al. (2003)].

Thermochemical H_2 R&D in the US lost its sense of urgency (and funding sources) and became near dormant in the mid-1980s. Later that decade, researchers at RWTH Aachen developed an alternative reactive distillation step for HI decomposition, based on the results of experiments showing H_2 could be obtained from HI without the latter first having to be separated from solution with I_2 and H_2O [Roth and Knoche (1989)]. This held the promise of a major improvement over the original General Atomics flowsheet. Not only did it lower the energy requirement, it also eliminated the need for phosphoric acid and the expensive vapor recompression equipment, leading the Germans to predict a 40% reduction in the cost of the H_2 product.

When interest in thermochemical H_2 R&D in the US was revived in the early 2000s, General Atomics initially proposed replacing phosphoric acid extraction in their flowsheet with Roth and Knoche's reactive distillation scheme. Based in part on the Germans' published calculations, they predicted net thermal efficiencies of 52% and higher [Brown et al. (2003)]. Attempts to duplicate Roth and Knoche's reactive distillation process using currently available process modeling tools, however, were unsuccessful. Further work by General Atomics' International Nuclear Energy Research Initiative (I-NERI) partner, the French Commissariat à l'Energie Atomique (CEA), indicated that the reactive distillation process actually required much more energy than the Germans had predicted [Goldstein et al. (2005)] – so much so, in fact, that heat pumps were needed to make the energy requirement comparable to that for phosphoric acid extraction. The heat pumps also dominate the capital cost of the reactive distillation process. The result is that the advantage over phosphoric acid extraction in terms of both efficiency and capital cost has been largely negated. A recently completed conceptual design of an SI cycle process using this flowsheet [Summers (2006)]

showed that over 75% of the capital cost of the H_2 plant was due to the HI decomposition section, with most of that attributable to the heat pumps. The net thermal efficiency of that flowsheet was found to be 46% (HHV basis).

Phosphoric acid extraction and reactive distillation are not the only options available for HI decomposition. The Japanese Atomic Energy Agency (JAEA) is developing a version of the SI process that uses electro-electrodialysis in conjunction with conventional distillation and a membrane reactor to concentrate and decompose HI [Kasahara et al. (2003)]. One reason for the difficulties with reactive distillation is that the concentration of HI in the I_2 rich phase of the product of the Bunsen reaction (10 mol% HI, 39 mol% I_2, and 51 mol% H_2O) is near that of the pseudo-azeotrope – and actually on the wrong side at temperatures below about 260°C. (The H_2O and HI binary forms a low boiling azeotrope that results in a pseudoazeotrope when combined with I_2 in a ternary solution.) Electro-electrodialysis is used in the JAEA flowsheet to increase the concentration of HI above its pseudoazeotrope so that it can be separated from solution with I_2 and H_2O by conventional distillation. Once purified, the HI is decomposed in a membrane reactor equipped with a H_2 permselective membrane that selectively removes H_2 product, helping drive the decomposition reaction forward. While this concept sounds good, the devil is in the details. The electro-electrodialysis process performs electrochemical work to concentrate HI in the catholyte, with inherent conversion losses, and membrane selectivities fall short. Recent estimates of the overall net thermal efficiency for the JAEA flowsheet are in the vicinity of 35% [Okuda et al. (2006)].

All three options for HI decomposition are being pursued to some extent in current SI process R&D programs worldwide.

Uncertainty about how best to accomplish HI decomposition is not the only unsolved technical challenge with the SI process. Among other things, materials issues, cross-contamination of HI and H_2SO_4 streams, high temperature heat transfer, and catalyst stability remain as major issues to be resolved.

SI cycle process streams are highly corrosive. At the relatively low temperature of the Bunsen reaction, fluoropolymer or glass linings allow the use of carbon steel for piping and vessels. However, the other two reactions occur at much higher temperatures, where metallic cladding or solid ceramics must be used instead. Only tantalum, niobium, and SiC have been found capable of withstanding direct contact with the $HI/I_2/H_2O$-containing streams of the HI decomposition section. No metal alloy has yet been found that can withstand boiling H_2SO_4 at elevated pressures. Thus, the issue of SI cycle materials remains an active area of research.

Cross-contamination of H_2SO_4 decomposition streams with iodine and HI decomposition streams with sulfur compounds is another area of concern. The three-phase split of the Bunsen reaction is not perfect. Concerns remain about how much residual cross-contamination can be allowed without adversely affecting corrosion and by-product formation.

The way in which heat from the high temperature heat source is transferred to the process poses a significant challenge and has direct bearing on the feasibility of Laser IFE as a heat

source for the SI cycle. The hottest temperatures occur in the H_2SO_4 decomposition section, at the outlet of the decomposition reactor. Obviously, heat transfer from the high temperature heat source would begin here. As the temperature of the heat transfer fluid decreases, the remaining heat could be used first to superheat the acid vapors entering the reactor, and then to vaporize the acid. Depending on how low the temperature of the coolant needs to go before returning to the IHX, the remaining heat could be used to concentrate the acid prior to decomposition, or could be used in the HI decomposition section to provide boil-up in the reactive distillation column.

Heat transfer to the H_2SO_4 decomposition reactor itself is an active area of research [Gelbard et al. (2006)]. The reaction, while favored thermodynamically, requires heterogeneous catalysis to proceed to any significant extent. Thus, the heat transfer fluid must supply heat not only to the acid vapor but also to the catalyst bed over which the decomposition reaction takes place. The highest temperatures considered here exceed the structural strength limitations of metal alloys, so ceramic materials, i.e. SiC_f/SiC, would have to be used. If helium were used as the heat transfer fluid, the coolant pressure would be on the order of 7-8 MPa, so the reactor would have to be capable of withstanding a large pressure differential (depending on the process-side pressure) at the temperature of the decomposition reaction while handling an extremely corrosive gas.

Finally, catalyst stability is a major concern at the high temperatures of the H_2SO_4 decomposition reaction. Sintering of the support as well as of the active sites, mobility of the active species, and accelerated deactivation processes can all come into play. This is another area of active research [Ginosar et al. (2006)].

Because the SI cycle faces a large number of technical challenges, some of which could ultimately prove to be insurmountable, attention is being given to alternate thermochemical cycles. The DOE NHI program has identified an alternative, hybrid cycle (HyS) that also makes use of sulfur oxidation and reduction. This cycle was originally identified as the most promising choice for development as a water-splitting process to be used with heat from an advanced, high temperature fission reactor. However, it was ultimately set aside in favor of the SI because it includes an electrochemical reaction step [Brown et al. (2000)].

5.1.2 Hybrid Sulfur Cycle

The Hybrid Sulfur (HyS) cycle shares one element in common with the SI cycle – the high temperature decomposition of H_2SO_4. In most other respects, however, it is quite different. HyS replaces two reaction steps, the Bunsen reaction and the decomposition of HI, with a single, electrochemical step. (See Figure 5-3.) It is this sulfur dioxide (SO_2)-depolarized electrolysis step that makes it a hybrid cycle.

The reversible cell potential for the SO_2-depolarized electrolyzer (SDE) at 25ºC is only 0.17 V in water, increasing to 0.29 V in 50-wt% H_2SO_4 in H_2O [Brecher et al. (1977)]. This is much less than the 1.23-V reversible cell potential for water at 25°C. In reality, water electrolyzers operate at cell potentials of 1.7 to 1.8 V when economically reasonable current densities are maintained. Ohmic losses and electrode overpotentials are responsible for this voltage increase. Likewise, SDEs in which the SO_2 is dissolved in 50 to 65 wt% H_2SO_4 are

expected to operate with cell potentials significantly greater than 0.29 V at practical current densities. In 1981, Lu et al. (1981) predicted cell potentials of 0.45 to 0.75 V at current densities of 100 to 400 mA/cm^2 when properly designed and optimized. The target of SRNL's current PEM electrolyzer development program is ≤ 0.6 V at 500 mA/cm^2 [Buckner et al. (2005)].

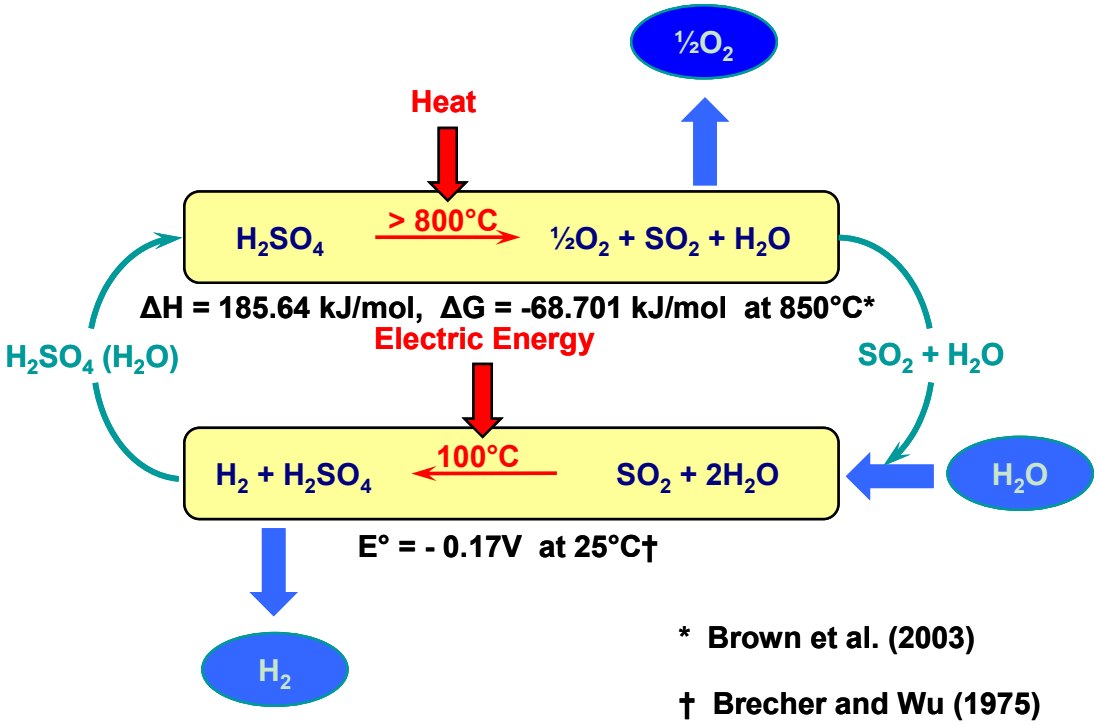

Figure 5-3 Hybrid Sulfur Cycle Schematic Diagram

Therefore, it is anticipated that the HyS electrolyzer will operate with a cell potential (and electrical requirement) roughly one-third to one-fourth that of a conventional water electrolyzer, permitting the creation of a high-efficiency water-splitting cycle possible. To be competitive with conventional low temperature electrolysis, the thermal energy required to effect the decomposition of H_2SO_4 needs to be substantially less than the thermal equivalent of the difference in cell potentials. Similarly, the thermal equivalent of the power requirement for the SDE has to be less than or equal to the thermal energy needed for HI decomposition in order for the HyS cycle to be competitive with the SI cycle. These criteria are easily satisfied as demonstrated by several complete flowsheets that have been prepared and previously published [Farbman (1976), Parker (1983), Buckner et al. (2005), and Gorensek et al. (2006)]. Estimated net thermal efficiencies for these flowsheets range from 45 to 54% (HHV basis).

HyS is the simplest known all-fluids thermochemical cycle, consisting of only the two reaction steps shown in Figure 5-3. No other all-fluids cycle proposed to date has less than three steps. Besides hydrogen and oxygen, sulfur is the only other element in the cycle, where it is alternately oxidized and reduced. This eliminates the cross-contamination concerns of the SI cycle.

The flowsheet for a HyS production plant powered by a Laser IFE heat source might look something like the simplified SI process flowsheet in Figure 5-2. Both cycles feature high temperature H_2SO_4 decomposition, which would be driven by heat supplied from the fusion heat source through a secondary coolant loop. One apparent difference is that the HyS cycle needs electric power for the SDE as well, so high temperature heat alone is insufficient.

Two options are available: one is to draw power for the SDE off the grid; the other is to use some of the heat from the Laser IFE heat source to generate power for the SDE. Figure 5-4 below is a block schematic illustrating the second option.

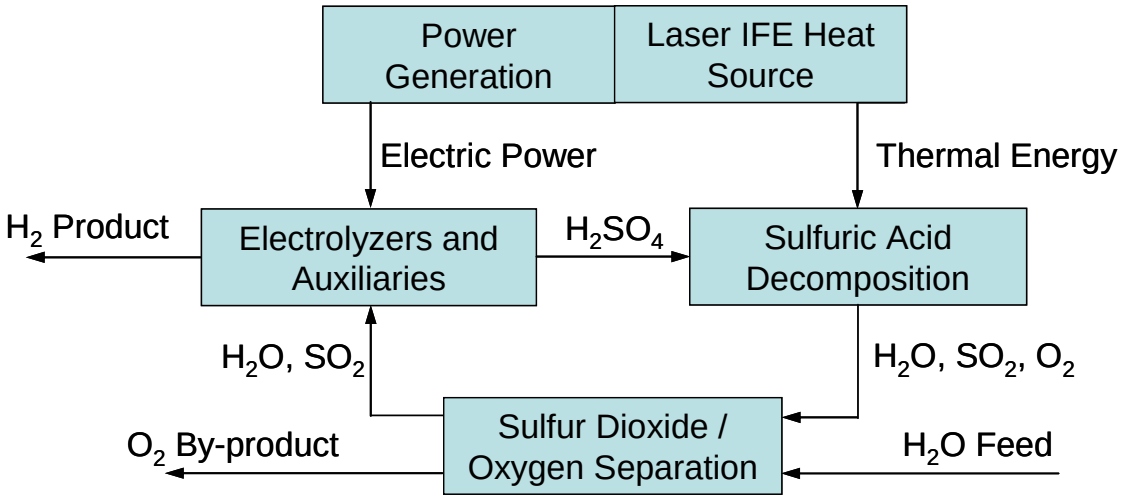

Figure 5-4 Simplified Block Flowsheet of Laser IFE-driven HyS Cycle Process

The idea here is that a portion of the self-cooled blanket would be used to generate electricity for the SDE and other power needs by rejecting heat to an efficient Brayton closed cycle gas turbine generator. The (larger) remainder of the blanket would reject heat to a secondary coolant loop that would then provide heat to the H_2SO_4 decomposition section.

It should be noted that current SI cycle flowsheets all have significant electricity demands. The reactive distillation of HI involves large heat pumps, while phosphoric acid extraction makes use of three-stage vapor recompression. (In fact, the reactive distillation heat pumps in the SI process draw slightly more power than the SDE in the HyS process on an equivalent hydrogen production basis [Summers (2006)].) Electro-electrodialytic concentration of HI also requires electric power. Thus the parallel production of electricity for captive use in the thermochemical production of hydrogen as in Figure 5-4 is an option for the SI cycle as well.

Although the HyS cycle is comprised of only two reaction steps, three process sections are shown in Figure 5-4. The third section, SO_2/O_2 Separation, is needed to remove O_2 product from the H_2O, SO_2, and O_2 effluent from H_2SO_4 decomposition. This can be accomplished by selective absorption of SO_2 into H_2O and H_2SO_4 [Buckner et al. (2005)].

Simplicity (two reactions instead of three), higher efficiency (up to 54% demonstrated vs. 47%) and elimination of HI/I_2 (and cross-contamination issues) from process streams are just

three of the advantages of the HyS cycle over the SI. Several others can be cited as well. For instance, the uncertainty of how best to accomplish HI decomposition is eliminated. HyS flowsheets can be designed and evaluated with a higher degree of certainty. Materials concerns are greatly simplified – only sulfur-species corrosion (common to both cycles) needs to be addressed. The SI cycle has to deal with iodine-species corrosion as well. The number of development hurdles for the HyS cycle is also smaller. Both cycles share the development of high temperature sulfuric acid decomposition as a common prerequisite. The only other development issue for HyS is the SDE. The SI cycle, however, depends on finding an efficient and economical way to decompose HI, on developing an effective implementation of the Bunsen reaction, and on successfully integrating the disparate pieces of the sulfur and iodine oxidation-reduction loops into a continuous process without cross-contamination.

Despite these numerous advantages, the HyS Cycle must still address the development of an effective, economical SDE, which is no trivial problem. Current efforts are focused on proton exchange membrane (PEM) electrolyzers [Steimke and Steeper (2006), Sivasubramanian et al. (2006)]. The key technology issues include: identifying or developing a PEM material that minimizes or eliminates SO_2 diffusion, achieving satisfactory membrane and electrocatalyst life, minimizing electrode overpotentials and ohmic losses (to achieve < 0.6 V cell potential at > 500 mA/cm^2 current density), and scale-up. SO_2 diffusion across the PEM from the anode to the cathode results in sulfur formation at the cathode, which, at best, is an efficiency loss (some of the power is used to reduce SO_2 to elemental sulfur instead of making H_2) and, at worst, can lead to poisoning of the cathode electrocatalyst. The membrane and catalytic anode and cathode need to be able to withstand continuous operation for years without excessive loss of performance. Cell design needs to provide for adequate mass transfer from the bulk electrolyte fluids to the electrodes while minimizing the resistance between the anode and cathode. All of these issues must be addressed in a design that provides adequate performance on a scale that can be incorporated into a massive hydrogen production facility.

Use of PEM technology for the HyS SDE gives some cause for optimism because of the huge R&D investment being made in automotive PEM fuel cells. Advances in automotive fuel cell technology will have spill-over benefits for the SDE. For example, minimization of neutral species transport is an active area of research for direct methanol fuel cells. PEM membranes that hinder diffusion of methanol will hinder diffusion of SO_2 as well. Membrane and catalyst life is as much an issue for vehicle fuels cells as it is for the SDE. Formulations that extend fuel cell life should also extend SDE life.

As for scale-up, it is worth noting that commercial chlor-alkali plants make chlorine and caustic on a massive scale using PEM electrolyzer technology. There is every reason to expect that PEM SDEs will be able to operate economically on a similar scale.

5.1.3 Other Cycles

At least 113 other thermochemical cycles have been proposed [Brown et al. (2000)]. These cycles either involve solid species, more reactions, and/or significantly lower or higher peak

temperatures, or they have not been sufficiently developed for evaluation, which is why they are not being included for consideration as water-splitting options for HAPL.

An example of a very high temperature thermochemical cycle that involves solids is the zinc-zinc oxide cycle, which is being actively developed for use with solar power. The high temperature reaction takes place at 2300K, achievable with highly concentrated sunlight, but well outside the practical limits for Laser IFE [Steinfeld (2002)].

One cycle that has been quite extensively studied is the Calcium-Bromine (Ca-Br) cycle [Doctor (2006)]. The 750°C peak temperature for Ca-Br is less than that for the sulfur cycles, and is limited by the melting point of calcium bromide. This cycle features gas-solid reactions in which the solid species are reactants as well as products. The current version is a modification of the original cycle, dubbed the UT-3 (for University of Tokyo – 3), which included reactions involving solid iron species [Tadokoro (1997)]. Efficiencies as high as 53% (HHV basis) have been claimed [Doctor (2006)], which is the reason why it has received considerable attention.

The principal technical issue for the Ca-Br cycle is the large volume change associated with the two gas-solid reactions involving calcium bromide and calcium oxide. This makes it difficult to maintain the integrity of the reaction beds and poses a major engineering challenge. It is primarily for this reason that the Ca-Br cycle is not included for consideration as a HAPL water-splitting option. The 750°C upper limit on reaction temperature would also prevent this cycle from taking full advantage of the higher temperatures possible with advanced blanket designs.

5.2 High Temperature Electrolysis

The final water-splitting option for HAPL is HTE, which takes advantage of the fact that, as temperature increases, the free energy change of the water-splitting reaction decreases, allowing more of the energy input to be in the form of heat instead of work. Predicted efficiencies for hydrogen production via HTE are comparable to those for thermochemical cycles [DOE (2005)]. A recent study estimated that the net thermal efficiency for a HTE process could be as high as 55% (HHV basis) [Stoots et al. (2005)].

HTE uses a device that could be construed as a solid oxide fuel cell (SOFC) operated in reverse to split water at high temperatures with a combination of electric and thermal energy. A schematic view of a typical HTE cell is shown in Figure 5-5 below. The cell consists of a solid oxide electrolyte, typically yttria-stabilized zirconia, sandwiched between two conducting electrodes. Cell thicknesses are on the order of 1 mm, with an electrolyte thickness between 10 and 100 μm. An equimolar mixture of steam and H_2 is introduced to the porous cathode at a temperature between 750 and 950°C. (The presence of H_2 helps maintain reducing conditions.) Electrons combine with H_2O molecules at the cathode, where oxide anions ($O^{=}$) are drawn into the electrolyte by the applied potential, releasing H_2 molecules. The $O^{=}$ anions are the charge carriers in the solid electrolyte, combining at the anode to release electrons and form O_2. A H_2 product containing roughly 25 mole percent water exits the cathode and passes through a separator where the water is removed and recycled. The operating pressure is expected to be 5 MPa [Herring et al. (2003)]. It should

be noted, however, that the current HTE development program is based on electrolyzers operating at atmospheric pressure. The development of high-pressure HTEs is a major challenge due to the ceramic components and the need for ceramic-to-ceramic sealing.

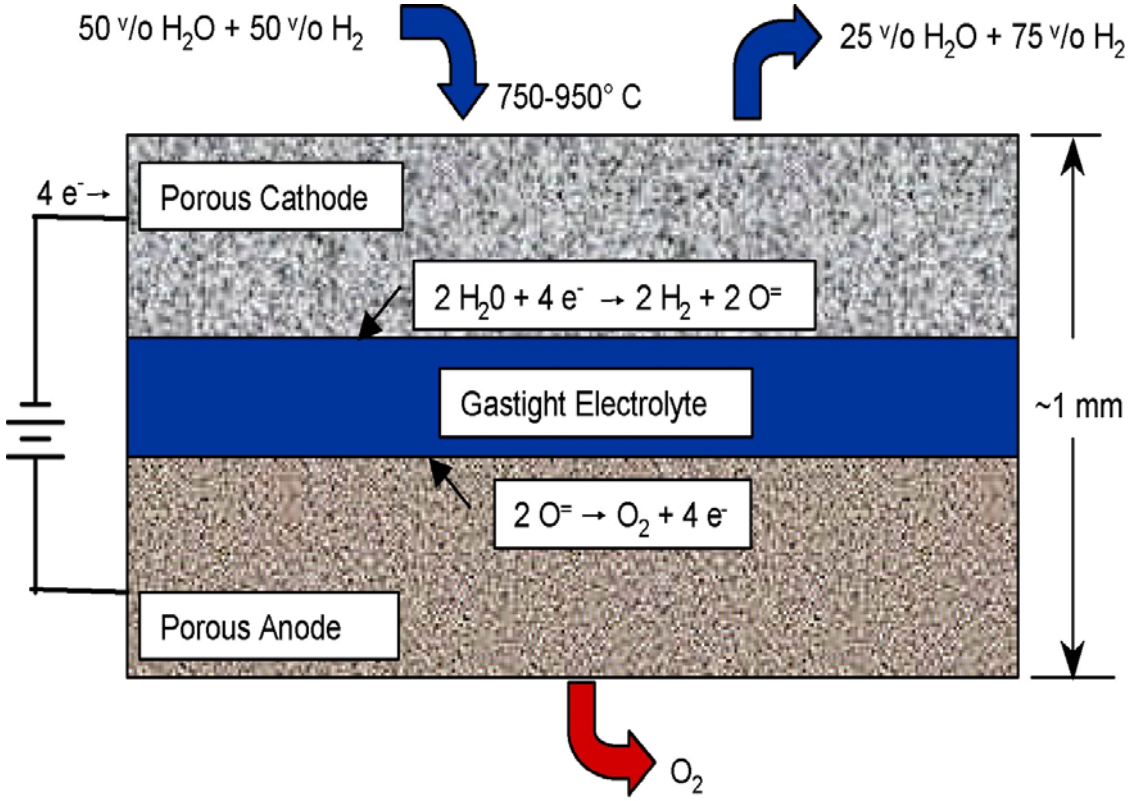

Figure 5-5 High Temperature Steam Electrolysis Cell Schematic [DOE (2004)]

HTE is built on SOFC technology and experience. The most highly developed SOFC designs uses tubular cell geometry, and tubular HTE designs are being pursued [Hoashi et al. (2006), Matsunaga et al. (2006)]. However, estimates of the hot volume required for hydrogen production using tubular HTE cells are ten times those for equivalent production with a planar configuration [DOE (2004)]. Consequently, the NHI is pursuing development of planar HTE cells. Because manufacturing processes cause shrinkage due to sintering, planar cells are currently constrained to be no larger than about 15 cm x 15 cm [Herring et al. (2003)]. Consequently, a water-splitting process using planar cell HTE coupled to a large heat source like a Laser IFE reactor would literally require millions of cells, all of which would need to be connected using high temperature gas manifolds. Electrical power and control connections would also have to be provided. Figuring out how to do this efficiently and economically is an active area of research [Herring et al. (2006)]. The development of larger size cells may be one of the most important challenges for a practical large-scale HTE hydrogen plant.

A simplified flowsheet depicting a Laser IFE heat source tied to a water-splitting process using HTE technology is depicted in Figure 5-6 below. The drawing is not accurate because it does not show the self-cooled blanket and secondary coolant loops. With that in mind,

what Figure 5-6 is intended to portray is something similar to the situation for HyS in Figure 5-4, although most of the heat carried by the blanket in this case would be used to generate electricity. The remainder of the heat would be used to provide superheated steam to the HTE at a temperature of 750 to 950°C and a pressure up to 5 MPa. Both steam and hydrogen would be present in the HTE feed in order to maintain reducing conditions.

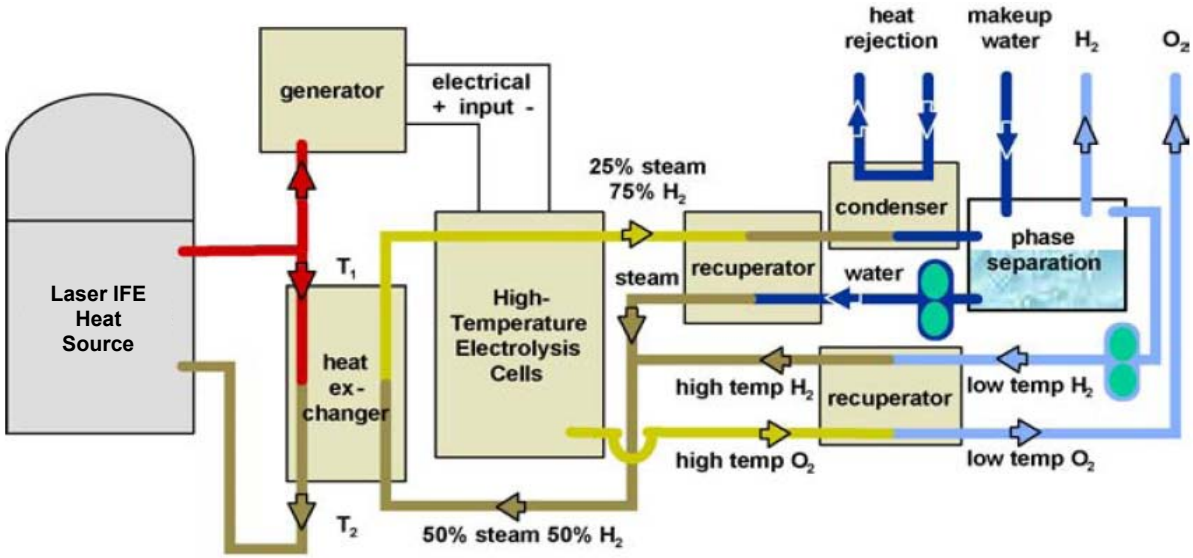

Figure 5-6 Simplified Flowsheet of Laser IFE-driven High Temperature Electrolysis Process [adapted from DOE (2004)]

Like the SI and HyS thermochemical cycles, HTE technology is still far from being ready for commercialization. A number of engineering issues need to be resolved first.

Planar cells currently use ceramic interconnections, which have higher resistivity and cost, and are more susceptible to thermal and mechanical shock than metallic interconnections. The use of metal connectors would be advantageous for these reasons, but is constrained by material temperature limits, which are significantly lower for metals than ceramics. The Idaho National Laboratory and Ceramatec Corp. are developing HTEs with metallic interconnects as part of the NHI program.

Unlike tubular cells, which physically separate the anodic and cathodic environments, planar cells rely on edge sealing to maintain separation. Sealing between cells is a major challenge. The sealant has to withstand both the reducing environment of the cathode and the oxidizing environment of the anode at HTE operating conditions. Given that literally millions of planar cells would be required for a commercial plant, this is a critical design problem.

The performance of the solid oxide electrolyte needs to be improved to allow higher current densities and/or lower operating temperatures (and less expensive materials). Higher conductivity materials that do not cost more to manufacture are being investigated. Candidate materials include scandium-doped zirconia and strontium-doped lanthanum gallate. Current cathode (nickel-zirconia cermet) and anode (strontium-doped lanthanum manganite) materials provide satisfactory performance, but also bear further research.

Alternative fabrication methods for planar cells that could provide cell sizes larger than 15 cm x 15 cm should be explored.

HTE will operate at high temperatures and pressures with steam and oxygen, mandating the use of corrosion-resistant alloys throughout the balance of plant. Therefore, materials of construction and their cost will be a major consideration and will influence the ultimate economic performance of a commercial plant.

5.3 Proposed Water-splitting Options for HAPL

Based on a review of available high temperature water-splitting technology, two options are recommended for further consideration as water-splitting methods that could be used with HAPL: the HyS thermochemical cycle, and HTE. The SI thermochemical cycle is not explicitly included in the remainder of this exercise, since it is unlikely that it would result in an improvement from the HyS cycle. Both the SI and HyS cycles would interact with a HAPL Laser IFE high temperature heat source primarily through the H_2SO_4 decomposition section of their operations, which are expected to be very similar. Both cycles would also benefit from efficient generation of electric power since their electricity demands are comparable. Thus, any analysis of the interaction with a HAPL heat source for one cycle would be directly applicable to the other. HyS was chosen over SI because it is simpler and far easier to model.

6.0 THE CASE FOR LASER IFE HYDROGEN PRODUCTION

Fusion energy is an intense source of high temperature heat that has much in common with fission energy. Both involve nuclear processes carried out in highly specialized equipment and require a significant capital cost investment. Fission reactors have been commercialized for several decades, so their capital cost and operating characteristics can be estimated with some certainty, even for new, advanced designs such as high temperature gas-cooled reactors. The same can not be said, however, for Laser IFE, which still faces years of development before commercialization. However, many of the technical and economic considerations that make generating hydrogen (by water-splitting) or generating electricity equally viable conduits for nuclear fission energy can be applied to the use of nuclear fusion in general, and Laser IFE in particular.

The HAPL program is developing Laser IFE technology with the goal of making a full-scale Laser IFE power plant a reality by the mid-to-late 2020s. Power will be generated by an advanced Brayton closed cycle gas turbine generator using high pressure helium as the working fluid. High temperature heat from the fusion reaction will be collected by the breeding blanket and transferred to the power conversion unit by means of a recirculating coolant. The same coolant that will provide energy to the power conversion unit could be used instead to provide heat to a high temperature water-splitting process like the HyS cycle or the HTE. As long as the water-splitting process can provide a continuous sink for fusion heat without any significant variation in coolant pressure drop or return temperature, the Laser IFE device will operate no differently whether it is attached to a power plant or to a water-splitting process.

Two different approaches for using high temperature heat to make hydrogen by splitting water are being proposed for HAPL. One, the HyS, is a thermochemical cycle that would operate like a typical, large, continuous chemical process. The other, HTE, would rely primarily on electricity generated by a parallel power conversion unit, and would use only a fraction of the Laser IFE source's thermal energy to heat the cells at a steady rate. Thus, both approaches could be coupled to a Laser IFE device without affecting its operation.

6.1 Temperature Considerations

Six blanket cases were established in Section 3.7. Four had been taken from self-cooled blanket conceptual designs that had been specifically prepared for HAPL, while the others were advanced concepts that had been developed for magnetic confinement devices.

Cases 1 and 5, with coolant outlet temperatures of 650°C and 700°C, respectively, would not be suitable for heating a dedicated water-splitting process. Case 1 is a self-cooled Li blanket for which safety considerations would mandate use of a secondary, anhydrous or inert coolant. That would imply two heat exchange operations between the heat source and the process, resulting in a peak process temperature below 600°C. Case 5 is a pressurized helium coolant that could, conceivably, be used without an intermediate coolant loop. The resulting peak process temperature could be between 650°C and 675°C, depending on the details of the helium-to-process heat exchange operation. If a secondary coolant loop were

used, the peak process temperature would drop to somewhere in the range of 600°C to 650°C. All of these peak temperatures are below the current operating range of the HTE process being developed for the NHI, which is between 750°C and 950°C. They are also below the 675°C kinetic limit [Brown et al. (2003)] for H_2SO_4 decomposition, i.e. the decomposition reaction does not proceed at an appreciable rate for reaction temperatures below this value. Therefore, Cases 1 and 5 are not suitable for high temperature water-splitting and will be dropped from further consideration. It should be noted that thermochemical cycles have been proposed that could make use of heat at these temperatures, and that steam electrolysis is possible at these temperatures as well. However, those technologies are not well-enough developed, and the likely net thermal efficiencies, $\eta_{p\ max}$., as shown in Table 4-1, are not very compelling.

Cases 2 and 3, with coolant outlet temperatures of 800°C and 799°C, respectively, would be acceptable for heating a HyS cycle process, but questionable for HTE. An inert secondary coolant loop would be required for safety reasons in both cases. That would imply a peak process temperature no higher than 750°C, and likely lower. The H_2SO_4 decomposition reaction kinetics could conceivably be fast enough, and the lower temperature might prolong catalyst life. That would make these blanket cases compatible with a HyS water-splitting process. One drawback is that the likely net thermal efficiencies, $\eta_{p,\ max}$., as shown in Table 4-1, would be limited to about 53% (HHV basis). A second drawback is that the lower peak operating temperature would reduce the yield in the H_2SO_4 decomposition reactor, requiring higher recycle rates and larger capital costs. As for HTE, 750°C is at the low limit of the current operating range. The performance of the HTE cell would be suboptimal unless a solid oxide electrolyte was specifically developed for lower temperatures. Lower temperature would also mean lower overall performance – lower efficiency for electricity generation and higher cell potential.

Cases 4 and 6, with coolant outlet temperatures of 930°C and 1,100°C, respectively, hold the greatest promise for coupling to a dedicated high temperature water-splitting process. The Case 4 blanket temperatures are nearly identical to the helium coolant temperatures for GA's H2-MHR reactor, a Generation IV design. Therefore, water-splitting processes being developed for the NHI would be a good match for a Case 4 blanket. As noted earlier, flowsheets for HyS and HTE at these conditions have been rated at up to 55% net thermal efficiency.

Case 6, which features a Pb-17Li blanket operating between 1,100°C and 800°C, could give Laser IFE a significant advantage over Generation IV fission reactors, because the latter are limited to coolant outlet temperatures of 900°C to 950°C. Electricity generation is more efficient at higher temperatures, which would benefit both HyS and HTE. More importantly, higher blanket temperature means higher peak process temperature, which favors H_2SO_4 decomposition equilibrium and kinetics. The only caveat is whether the materials exist to hold the H_2SO_4 decomposition catalyst in sulfuric acid vapor while being heated by a molten salt or pressurized helium heat transfer fluid at these temperatures, and whether the catalyst can withstand the high temperature (1,000°C to 1,050°C).

In summary, blanket temperatures above 800°C to 850°C would be suitable for coupling a Laser IFE device with a high temperature water-splitting process like HyS or HTE. In general, the higher the temperature, the better, subject to materials constraints.

6.2 Heat Transfer Considerations

Laser IFE blanket coolants can achieve sufficient temperatures to supply heat to a high temperature water-splitting process like HyS or HTE. However, with the exception of helium coolants, they are not suitable for direct heat transfer because they contain molten Li metal that reacts violently with water and other compounds. A leak between a Li metal-containing coolant and the H_2O-containing process stream in a heat exchanger could have disastrous consequences. Therefore, an intermediate coolant loop is almost a certain requirement.

Candidate materials for the intermediate loop coolant include pressurized helium, molten salts, and molten metals. Of all the possibilities, molten fluoride salts appear to hold the greatest promise for the temperature range being considered [Forsberg (2006)]. In particular, the ternary eutectic salt mixture 46.5% lithium fluoride, 11.5% sodium fluoride, 42% potassium fluoride, known as FLiNaK, has the best overall heat transfer characteristics [Williams (2006)].

The NHI is developing water-splitting technology for use with advanced gas-cooled fission reactors like GA's H2-MHR. Because the primary coolant in all of the leading reactor designs is pressurized helium, the secondary heat transfer fluid circulating between the reactor and the water-splitting process will most likely be pressurized helium also. That is because use of identical fluids at similar conditions on either side of the IHX greatly simplifies its design and operation. Helium is also chemically inert, even at the 900°C to 950°C temperatures of advanced gas-cooled fission reactors.

This could give Laser IFE another significant edge over Generation IV fission technology, because the heat transfer characteristics of molten salt are significantly better than those of pressurized helium. That advantage would manifest itself in several ways.

Current NHI H_2SO_4 decomposition process concepts reflect operation at high pressures (7 MPa or higher) to balance the pressure of the helium heat transfer medium [e.g. Summers (2006)]. However, the H_2SO_4 decomposition equilibrium is favored by lower pressure. Molten salt coolants need only have enough pressure to overcome frictional losses in the process equipment and piping, allowing operation of the decomposition process at much more favorable pressures. Consequently, a Laser IFE-driven HyS cycle could have a molten salt-heated H_2SO_4 decomposition reactor operating at significantly lower pressure, giving higher per-pass conversion, lower capital cost, and more efficient operation.

Better heat transfer characteristics for molten salt could result in smaller temperature differences in the high temperature exchangers. That would mean slightly higher process temperatures for Laser IFE than Generation IV, given the same heat source temperature. That would favor the H_2SO_4 decomposition equilibrium. Smaller temperature differences

would also make better use of availability, so the overall process net thermal efficiency would be marginally improved.

Finally, the energy density of molten salt is a couple of orders of magnitude higher than that for pressurized helium. A molten salt coolant like FLiNaK flowing at pressures under 1 MPa would require much smaller process equipment (piping, valves, heat exchangers, etc.) than helium at 7 MPa, so the cost of the high-temperature-heat-source-to-process heat transfer equipment could be considerably less for Laser IFE fusion than for Generation IV fission reactors.

6.3 Materials Considerations

Use of a molten salt coolant like FLiNaK at temperatures approaching 1,100°C raises the obvious specter of severe corrosion. However, the high temperature streams of the water-splitting processes have serious corrosion concerns of their own. Consequently, advanced corrosion-resistant materials like SiC (which would be a candidate for handling FLiNaK), are already being investigated for use in high temperature heat transfer applications for the NHI. One example is the H_2SO_4 decomposition reactor design being developed at Sandia National Laboratories (SNL), which is shown in Figure 6-1 below.

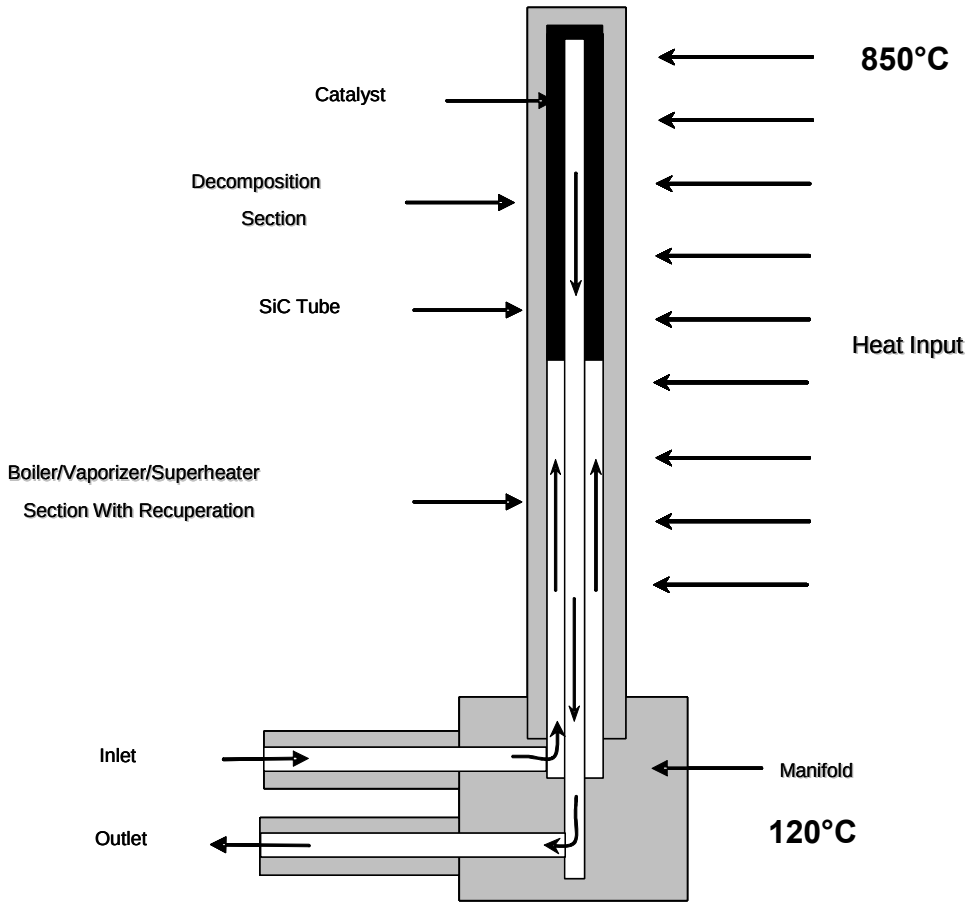

Figure 6-1 SNL SiC H_2SO_4 Decomposition Reactor Concept [Evans (2006)]

This concept features a "bayonet" reactor made of SiC that would be immersed in the high temperature heat transfer fluid (pressurized helium in the intended application) with the seal maintained at lower temperature. The operating details can be found elsewhere [Gelbard et al. (2006)].

What is important to note here is that while using molten salt at high temperatures does pose a serious materials problem, creative ways of dealing with those problems are possible, using advanced materials. Furthermore, some screening work has already been done for molten salt coolants at temperatures relevant for NHI water-splitting processes (up to 950°C) [Williams (2006)].

The Laser IFE technology being developed for the HAPL program is capable of achieving heat transfer fluid temperatures as high as 1,100°C. To take full advantage of this energy source, materials capable of handling molten salts at temperatures up to 1,100°C will have to be identified and validated. While not a trivial task, there is every reason to expect that this can be done within the time frame of the HAPL program.

7.0 SUITABILITY OF FTF FOR HYDROGEN PRODUCTION DEMONSTRATION

The purpose of the FTF is to serve as a test bed for fusion power plant materials and components. If hydrogen production by water-splitting is intended to be a part of the HAPL program, then it would be appropriate to consider FTF as a potential test bed for hydrogen production plant materials and components as well.

Flexibility in start-up, testing, and operation is provided by the fact that an actual operating Laser IFE device is not needed to demonstrate the feasibility or commercial viability of splitting water with heat from a fusion energy source. The energy source and the hydrogen process will be connected only through the intermediate coolant loop in a real application. For the purpose of initial testing of the Laser IFE device, the hydrogen process could be replaced by an equivalent heat sink connected to the intermediate coolant loop with no discernible effect on its operation. Similarly, the water-splitting process would operate no differently if the Laser IFE device were replaced with an equivalent heat source. Therefore, demonstration of the feasibility of water-splitting using a Laser IFE heat source could actually be achieved with separate demonstrations of the two components.

However, a significant advantage of including a hydrogen production demonstration as part of FTF is that it forces the development of water-splitting technology to a matching schedule, and sets the bar for success at a higher level than might be the case for a stand-alone process. A combined Laser IFE/H_2 production demonstration also provides a tangible end product that clearly demonstrates the technical feasibility of the process.

The thermal energy output of the FTF device is projected to be 150 MW_{th} [Obenschain et al. (2006)]. Only a fraction of this energy would be needed for a successful hydrogen production demonstration. For example, the JAEA is planning construction and operation of a 1,000-m^3/hr engineering scale demonstration thermochemical hydrogen production plant that will be driven by a 30-MW_{th} gas cooled reactor by 2015 [WNA (2006)]. Assuming a net thermal efficiency of 35% (HHV basis), that corresponds to a roughly 10-MW_{th} heat input. In the US, DOE-NE is planning to build a 50-MW_{th} high temperature hydrogen production demonstration plant in conjunction with the Next Generation Nuclear Plant (NGNP) by 2017 [DOE (2004)].

Simulation-based chemical process design tools available today make scale-up much more straightforward than in the past. A 10- to 50-MW_{th} demonstration plant successfully operated and credibly documented should be sufficient to convince industry of the commercial viability of the technology. Consequently, the FTF should be suitable for a hydrogen production demonstration.

8.0 CONCLUSIONS AND RECOMMENDATIONS

Based on the work described in this report, the following conclusions can be drawn:

- Laser IFE provides high temperature heat that could be used to drive a water-splitting hydrogen production process with reasonable net thermal efficiency. Both HyS/SI and HTE technologies could be coupled with Laser IFE heat and power technology.
- Laser IFE is capable of generating blanket coolant temperatures up to 1,100°C using a molten Pb-17Li self-cooled blanket and SiC_f/SiC FW and blanket structure. This is about 150°C hotter than Generation IV fission technology.
- Laser IFE using a molten Pb-17Li self-cooled blanket has an advantage over pressurized helium-cooled Generation IV fission technology because it can be more easily used with a low pressure molten salt secondary coolant. Consequently, it allows the H_2SO_4 decomposition reactor to operate at lower pressures and higher temperatures than in processes developed for the NHI.

The following recommendations are made:

- Further study should be conducted to quantify the differences between hydrogen cycles powered by fusion versus fission heat sources.
- A preconceptual design, including a process flowsheet and material/energy balances, should be created for a 10- to 50-MW_{th} water-splitting process integrated with the FTF.

9.0 REFERENCES

Besenbruch, G.E., "General Atomic Sulfur-Iodine Thermochemical Water-Splitting Process," Am. Chem. Soc., Div. Pet. Chem., Prepr., **271**, 48 (1982).

Boccaccini, L.V., Fischer, U., Gordeev, S., and Malang, S., "Advanced helium cooled pebble bed blanket with SiC_f/SiC as structural material", *Fusion Engineering and Design*, **49-50**, 491-497, (2000).

Brecher, L.E., Spewock, S., and Warde, C. J., "The Westinghouse Cycle for the Thermochemical Decomposition of Water", *Int. J. Hydrogen Energy*, **2**, 7, 1977.

Brecher, L.E., and Wu, C.K., "Electrolytic decomposition of water", Westinghouse Electric Corp., Patent 3,888,750, June 10, 1975.

Brown, L.C., Funk, J.F., and Showalter, S.K., "High Efficiency Generation of Hydrogen Fuels Using Nuclear Power", Report No. GA-A23451, General Atomics Corp., July, 2000.

Brown, L.C., Besenbruch, G.E., Lentsch, R.D., Schultz, K.R., Funk, J.F., P.S. Pickard, Marshall, A.C., and Showalter, S.K., "High Efficiency Generation of Hydrogen Fuels Using Nuclear Power", Report No. GA-A24285, General Atomics Corp., June, 2003.

Buckner, M.B., Adams, T.M., Gorensek, M.B., Hamm, L.L., Hassan, N.M., Hobbs, D.T., Nash, C.A., Qureshi, Z.H., Steeper, T.J., Steimke, J.L., and Summers, W.A., "Conceptual Design for a Hybrid Sulfur Hydrogen Production Plant", Report No. WSRC-TR-2004-00460, Rev. 0, Savannah River National Laboratory, April 1, 2005.

Doctor, R.D., "Evaluation of a Continuous Calcium-Bromine Thermochemical Cycle", PD16, DOE Hydrogen Program 2006 Annual Merit Review Proceedings, Arlington, VA, May 16, 2006.

Evans, R.J., "Nuclear Hydrogen Initiative Thermochemical Cycles", AIChE Spring National Meeting, Orlando, FL, April 24, 2006.

Farbman, G.H., "The Conceptual Design of an Integrated Nuclear-hydrogen Production Plant Using the Sulfur Cycle Water Decomposition System", NASA Contractor Report, NASA-CR-134976, 1976.

Forsberg, C.W., "Developments in Molten Salt and Liquid-Salt-Cooled Reactors", Paper 6292, Proceedings of ICAPP '06, Reno, NV, June 4–8, 2006

Gelbard, F., Moore, R. C., Vernon, M.E., Parma, E.J., Rivera, D.A., Stone, H.B. J., Andazola, J.C., Naranjo, G.E., and Pickard, P.S., "Sulfuric Acid Decomposition with Heat and Mass Recovery Using a Direct Contact Exchanger", 230b, AIChE 2006 Annual Meeting, San Francisco, CA, November 14, 2006.

Ginosar, D.M., Rollins, H.W., Petkovic, L.M., and Burch, K.C., "Sulfuric Acid Decomposition Catalysts and Reaction Considerations for Sulfur-Based Thermochemical Water Splitting Cycles", 182c, AIChE Spring National Meeting, Orlando, FL, April 26, 2006.

Goldstein, S., Borgard, J.-M., and Vitart, X., "Upper bound and best estimate of the efficiency of the Iodine sulphur cycle", *Int. J. Hydrogen Energy*, **30**, 619-626 (2005).

Gorensek, M.B., Summers, W.A., and Eargle, J.A., "Expected Performance of Hybrid Sulfur Process Based on SO_2-Depolarized Electrolyzer Technology", Report No. WSRC-STI-2006-00136, Rev. 0, Savannah River National Laboratory, August 30, 2006.

Hermsmeyer, S., "Improved Helium Cooled Pebble Bed Blanket", Report No. FZKA 6399, Forschungszentrum Karlsruhe GmbH, Karlsruhe, Germany (1999).

Herring, J.S., Lessing, P., O'Brien, J.E., Stoots, C., Hartvigsen, J., and Elangovan, S., "Hydrogen Production through High-Temperature Electrolysis in a Solid Oxide Cell", Nuclear Production of Hydrogen, OECD Second Information Exchange Meeting, Argonne, IL, October 3, 2003.

Herring, S., O'Brien, J., Stoots, C., Hawkes, G., McKellar, M., Sohal, M., Harvego, DeWall, K., Hall, D., Hartvigsen, J., Elangovan, S., Larsen, D., Petri, M., Myers, D., Yildiz, B., Carter, D., and Doctor, R., "Laboratory-Scale High Temperature Electrolysis System", PD17, DOE Hydrogen Program 2006 Annual Merit Review Proceedings, Arlington, VA, May 17, 2006.

Hoashi, E., Ogawa, T., Matsunaga, K., Nakada, K., Fujiwara, S., Kasai, S., "Simulation Modeling of a Tubular-type Solid Oxide Electrolysis Cell for Hydrogen Production on Nuclear Power Plant", International Congress on Advances in Nuclear Power Plants, Reno, NV, June 6, 2006.

Ihli, T., "DEMO Fusion Core Engineering: Blanket Integration and Maintenance", US/Japan Workshop on Power Plant Studies and Advanced Technologies with EU participation, San Diego, CA, January 25, 2006.

"ITER", http://www.iter.org/index.htm, October 9, 2006.

Kasahara, S., Hwang, G.-J., Nakajima, H., Choi, H.-S., Onuki, K., and Nomura, M., "Effects of Process Parameters of the IS Process on Total Thermal Efficiency to Produce Hydrogen from Water", *J. Chem Eng. Japan*, **36**(7), 887-899 (2003).

Knoche, K.-F. and Funk, J.E., "Entropy production, efficiency, and economics in the thermochemical generation of synthetic fuels. I. The hybrid sulfuric acid process", *Int. J. Hydrogen Energy*, **2**, 377-385 (1977).

Lu, P.W.T., Garcia, E.R., Ammon, R.L., "Recent developments in the technology of sulphur dioxide depolarized electrolysis", *J. Appl. Electrochem.*, **11**, 347-355, 1981.

Matsunaga, K., Hoashi, E., Fujiwara, S., Yoshino, M., Ogawa, T., Kasai, S., "Hydrogen Production System with High Temperature Electrolysis for Nuclear Power Plant", International Congress on Advances in Nuclear Power Plants, Reno, NV, June 6, 2006.

Morley, N. et al., "MHD Modeling and Experiments at UCLA for the ITER Test Blanket Program", Plasma Facing Components Meeting, Princeton, NJ, May 10, 2005.

National Research Council, The Hydrogen Economy: Opportunities, Costs, Barriers, and R&D Needs, Washington, DC: National Academies Press, 2004.

Norman, J.H., Russell, J.L., Jr., Porter, J.T., II, McCorkle, K.H., Roemer, T.S., and Sharp, R., "Process for the Thermochemical Production of Hydrogen", General Atomic Co., Patent 4,089,940, May 16, 1978.

Norman, J.H., Besenbruch, G.E., Brown, L.C., O'Keefe, D.R., and Allen, C.L., "Thermochemical water-splitting cycle, bench-scale investigations, and process engineering" Report No. GA-A16713, General Atomic Co., May 1982.

Obenschain, S., "A New Path to Laser Fusion Energy", Technical Review, United States Naval Research Laboratory, May 3, 2006.

Obenschain, S.P., Colombant, D. G., Schmitt, A. J., Sethian, J. D., and McGeoch, M. W., "Pathway to a lower cost high repetition rate ignition facility", *Physics of Plasmas*, **13**(5) 056320 (2006).

Okuda, H., Yamaki, T., Kubo, S., and Onuki, K., "Improvement of the Thermal Efficiency of Hydrogen Iodide Concentration in I-S Process by Using Radiation-grafted Membrane in Electrolysis System", 182d, AIChE Spring National Meeting, Orlando, FL, April 26, 2006.

Parker, G.H., "Solar Thermal Hydrogen Production Process", Final Report from Westinghouse Electric Corp. to US DOE, DOE/ET/20608-1, 1983.

Princeton Plasma Physics Laboratory, ITER and the Promise of Fusion Energy, pamphlet February 2006.

Raffray, A.R., "Advanced Chamber Concept with Magnetic Intervention: Ion Dump Issues, Status of Blanket Study", 15th HAPL Program Workshop, La Jolla, CA, August 9, 2006.

Raffray, A.R., email communication, October 27, 2006.

Raffray, A.R., El-Guebaly, L., Malang, S., Sviatoslavsky, I., Tillack, M.S., Wang X., and the ARIES Team, "Advanced power core system for the ARIES-AT power plant", *Fusion Engineering and Design*, **80**, 79-98, (2006).

Roth, M., and Knoche, K.F., "Thermochemical Water-splitting through Direct HI Decomposition from $H_2O/HI/I_2$ Solutions", *Int. J. Hydrogen Energy*, **14**, 545-549 (1989).

Scott, D.S., "Energy Currencies" *Int. J. Hydrogen Energy*, **19**(3), 199-201 (1994).

Sethian, J.D. et al., "Fusion Energy with Lasers, Direct Drive Targets and Dry Wall Chambers," *Nuclear Fusion*, **43**,1693-1709 (2003).

Sethian, J. personal communications, September 18 through October 30, 2006.

Sethian, J. and Obenschain, S., "Fusion Energy with Lasers, Direct Drive Targets, and Solid Wall Chambers", Fusion Power Associates Annual Meeting, Washington, DC, November 19-21, 2003.

Sethian, J. and Obenschain, S., "Laser Fusion Energy: Progress in HAPL and Introducing The Fusion Test Facility", Fusion Power Associates Annual Meeting, Washington, DC, October 12, 2005.

Sivasubramanian, P.K., Ramasamy, R.P., Freire, F.J., Holland, C.E., and Weidner, J.W., "Electrochemical hydrogen production from thermochemical cycles using a proton exchange membrane electrolyzer", *Int. J. Hydrogen Energy*, in press (2006).

Steimke, J.L. and Steeper, T.J., "Characterization Testing and Analysis of Single Cell SO_2 Depolarized Electrolyzer", Report No. WSRC-STI-2006-00120, Rev. 0, Savannah River National Laboratory, August 30, 2006.

Steinfeld, A., "Solar Hydrogen Production Via a Two-step Water-splitting Thermochemical Cycle Based on Zn/ZnO Redox Reactions", *Int. J. Hydrogen Energy*, **27**(6), 611-619 (2002).

Stoots, C., O'Brien, J., McKellar, M., Hawkes, G., and Herring, J.S., "Engineering Process Model for High-Temperature Steam Electrolysis System Performance Evaluation", 348a, AIChE Annual Meeting, Cincinnati, OH, November 2, 2005.

Sviatoslavsky, I.N., Raffray, A.R., Sawan, M.E., and Wang, X., "A Lithium Self-Cooled Blanket for the HAPL Conceptual Inertial Confinement Reactor", *Fusion Science & Techn.*, **47**(3), 535-539, (2005).

Sviatoslavsky, G., "Blanket Design for a Magnetic Diversion Chamber", 14th HAPL Program Workshop, Oak Ridge, TN, March 22, 2006.

Summers, W.A., "Centralized Hydrogen Production from Nuclear Power: Infrastructure Analysis and Test-Case Design Study – Final Project Report, Phase B Test-Case Preconceptual Design", Report No. WSRC-MS-2005-00693, Rev. 0, Savannah River National Laboratory, April 28, 2006.

Tadokoro, Y., Kajiyama, T., Yamaguchi, T., Sakai, N., Kameyama, H., and Yoshida, K., "Technical Evaluation of UT-3 Thermochemical Hydrogen Production Process for an Industrial Scale Plant," *Int. J. Hydrogen Energy*, **22**(1), 49-56 (1997).

Tillack, M.S. et al., "Fusion power core engineering for the ARIES-ST power plant," *Fusion Engineering and Design*, **65**, 215-261, (2003).

United States Department of Energy, Nuclear Energy Research Advisory Committee, A Technology Roadmap for Generation IV Nuclear Energy Systems, 03-GA50034, December 2002.

United States Department of Energy, Office of Nuclear Energy, Science and Technology, Nuclear Hydrogen R&D Plan, March 2004.

United States Department of Energy, Office of Nuclear Energy, Science and Technology, Nuclear Hydrogen Initiative, Ten Year Program Plan, March 2005.

United States Department of Energy, Annual Energy Review 2005, Report No. DOE/EIA-0384(2005), July 27, 2006.

University of California, San Diego, "The High Average Power Laser Program", http://www-ferp.ucsd.edu/HAPL/, October 9, 2006.

Williams, D.F., "Assessment of Candidate Molten Salt Coolants for the NGNP/NHI Heat-Transfer Loop", Report No. ORNL/TM-2006/69, Oak Ridge National Laboratory, June, 2006.

Wong, C.P.C., Malang, S., Nishio, S., Raffray, R., and Sagara, S., "Advanced High Performance Solid Wall Blanket Concepts", Report No. GA-A23900, General Atomics Corp., April, 2002.

World Nuclear Association, "Nuclear Power in Japan, September 2006", http://www.world-nuclear.org/info/inf79.htm, November 2, 2006.